the phosphatidylinositol 3-kinase (PI3K)/Akt-dependent pathway.

Methods

Reperfusion Model

We used male Sprague-Dawley rats (Japan SLC Inc, Hamamatsu, Japan) weighing 180 to 220 g. Ligation of the left coronary artery was performed as described previously.[11] In brief, under anesthesia with pentobarbital sodium (30 mg/kg) and artificial ventilation, the heart was exposed via left thoracotomy, and the left coronary artery was ligated 2 to 3 mm from its origin between the pulmonary artery conus and the left atrium with a 6-0 Prolene suture. The heart was subjected to regional ischemia for 30 minutes, followed by coronary reperfusion through release of the tie. After ligation of the left coronary artery, AM (0.05 $\mu g \cdot kg^{-1} \cdot min^{-1}$), AM plus wortmannin (16 μg/kg intravenous injection 15 minutes before AM infusion; a PI3K inhibitor),[12] or placebo (0.9% saline) was administered for 60 minutes through a catheter inserted into the left jugular vein. Sham-operated rats only underwent left thoracotomy. The chest wall was then closed, and the animal was allowed to recover. This protocol resulted in the creation of 4 groups: sham-operated rats (sham group, n=12), placebo-treated rats with ischemia/reperfusion (I/R-placebo group, n=19), AM-treated rats with ischemia/reperfusion (I/R-AM group, n=19) and AM plus wortmannin–treated rats with ischemia/reperfusion (I/R-Wo+AM group, n=15).

All animal experiments were conducted in accordance with the principles and procedures outlined in the *National Cardiovascular Center Guide for the Care and Use of Laboratory Animals*, which adheres strictly to the National Institutes of Health animal experimental guidelines, with the approval of the National Cardiovascular Center Animal Experimental Committee.

Hemodynamic Studies

We performed hemodynamic measurements 24 hours after ischemia/reperfusion. A 1.5F micromanometer-tipped catheter was advanced into the left ventricle through the right carotid artery, and a polyethylene catheter (PE-50) was advanced into the right ventricle through the right jugular vein to measure right ventricular pressure. Heart rate was also monitored with an ECG.

Measurement of Plasma AM Level

Blood samples were obtained from the right carotid artery during 0.05 $\mu g \cdot kg^{-1} \cdot min^{-1}$ AM infusion. Plasma AM level was measured by immunoradiometric assay, as described previously.[8,11]

Assessment of Infarct Size

After hemodynamic measurements, the heart was removed and perfused with a Langendorff apparatus for 10 minutes to wash out the blood and then fixed with 10% neutral buffered formalin. The heart was sliced transversely from the apex to the atrioventricular groove in 2.5-mm thicknesses and weighed separately. Within 24 hours after fixation, each section was embedded in paraffin. Serial 5-μm myocardial sections were cut with microtome and mounted on siliconized slides. After Masson trichrome staining, infarct size of each slice was analyzed by microscopy. Myocardial coagulation necrosis could be distinguished from viable myocardium as a definite alteration of staining, and then the infarct area was outlined and measured by planimetry. Infarct weight was determined with the following equation: % infarct area × weight of each slice, as described previously.[13] Finally, we determined percent infarct size as total infarct weight divided by total left ventricular (LV) weight.

TUNEL Staining

Hearts were isolated from each group (n=5) 6 hours after reperfusion for the terminal dUTP nick-end labeling (TUNEL) assay. After the blood and the fixation were washed out, the heart was also sliced transversely in 2.5-mm thicknesses. Paraffin-embedded, 5-μm-thick myocardial sections were used as described previously.[14] In brief, after deparaffinization and enzyme-mediated antigen retrieval, TUNEL staining was performed with a commercially available kit (Apop Tag Plus, Intergen). Samples were incubated with monoclonal anti-desmin antibody (Sigma) followed by tetramethylrhodamine isothiocyanate-conjugated rabbit anti-mouse antibody (DAKO). Counterstaining was performed with propidium iodide. Finally, these slides were mounted with Vector Shield (Vector Laboratories) containing an antifade reagent. We measured the number of TUNEL-positive nuclei in myocytes by means of confocal microscopy (Olympus, Fluoview 500). Quantitative analysis was performed on 60 high-power fields (magnification ×600) with at least 10 randomly selected fields used per section. We counted the number of cardiomyocytes at least $>10^4$ cells per heart.

DNA Ladder Assay

We used 10 additional rats for the DNA ladder assay (sham group, n=2; I/R-placebo group, n=4; I/R-AM group, n=4). Rats were killed, and the heart was excised 24 hours after ischemia/reperfusion. Immediately before heart isolation, 1% Evans blue was infused slowly into the left ventricle to delineate the risk area after coronary religation. Then, 40 mg of myocardium in the posterolateral border zone between the nonrisk area and the risk area was resected. Each specimen was frozen in liquid nitrogen and stored at −80°C until DNA extraction. DNA extraction and electrophoresis were performed with a commercially available kit (Apoptosis Ladder Detection Kit, WAKO).

Immunohistochemical Analysis

To assess localization of calcitonin receptor-like receptor (CRLR), a receptor for AM, in cardiac tissues, we performed immunohistochemical analysis using rabbit anti-rat CRLR antibody (Zymed). Localization of Akt phosphorylation was examined with rabbit anti-rat phospho-Akt antibody (Cell Signaling).

Western Blot Analysis

To identify Akt phosphorylation in myocardial tissues after AM infusion, Western blotting was performed with a commercially available kit (PhosphoPlus Akt [Ser 473] antibody kit, Cell Signaling). Myocardial tissues were obtained from rats treated with intravenous AM (0.01, 0.05, and 0.25 $\mu g \cdot kg^{-1} \cdot min^{-1}$), AM (0.05 $\mu g \cdot kg^{-1} \cdot min^{-1}$) plus wortmannin (16 μg/kg intravenous injection 15 minutes before AM infusion), or saline for 60 minutes during ischemia/reperfusion. These samples were homogenized on ice in a 0.1% Tween 20 homogenization buffer with a protease inhibitor (Complete, Roche). After centrifugation for 20 minutes at 4°C, the clear supernatant was used for Western blot analysis. Protein concentration was measured by Bradford's method (Bio-Rad). Fifty micrograms of each protein extract were transferred in sample buffer, loaded on 7.5% SDS-polyacrylamide gel, and blotted onto nitrocellulose membrane (Bio-Rad) with a wet blotting system. After being blocked for 60 minutes, the membranes were incubated with primary antibodies in blocking buffer (1:500) at 4°C overnight. Antibodies were used at the manufacturer's recommended dilution (Cell Signaling). The membranes were incubated with secondary antibodies, which were conjugated with horseradish peroxidase (Cell Signaling), at a final dilution of 1:2000. Signals were detected with LumiGLO chemiluminescence reagents (Cell Signaling).

Statistical Analysis

All data are expressed as mean±SEM unless otherwise indicated. Comparisons of parameters among the 3 or 4 groups were made by 1-way ANOVA for repeated measures, followed by Scheffé test. A probability value <0.05 was considered to indicate statistical significance.

Results

Reduction of Myocardial Infarct Size After AM Infusion

Moderate to large infarcts were observed in Masson trichrome–stained myocardial sections 24 hours after ische-

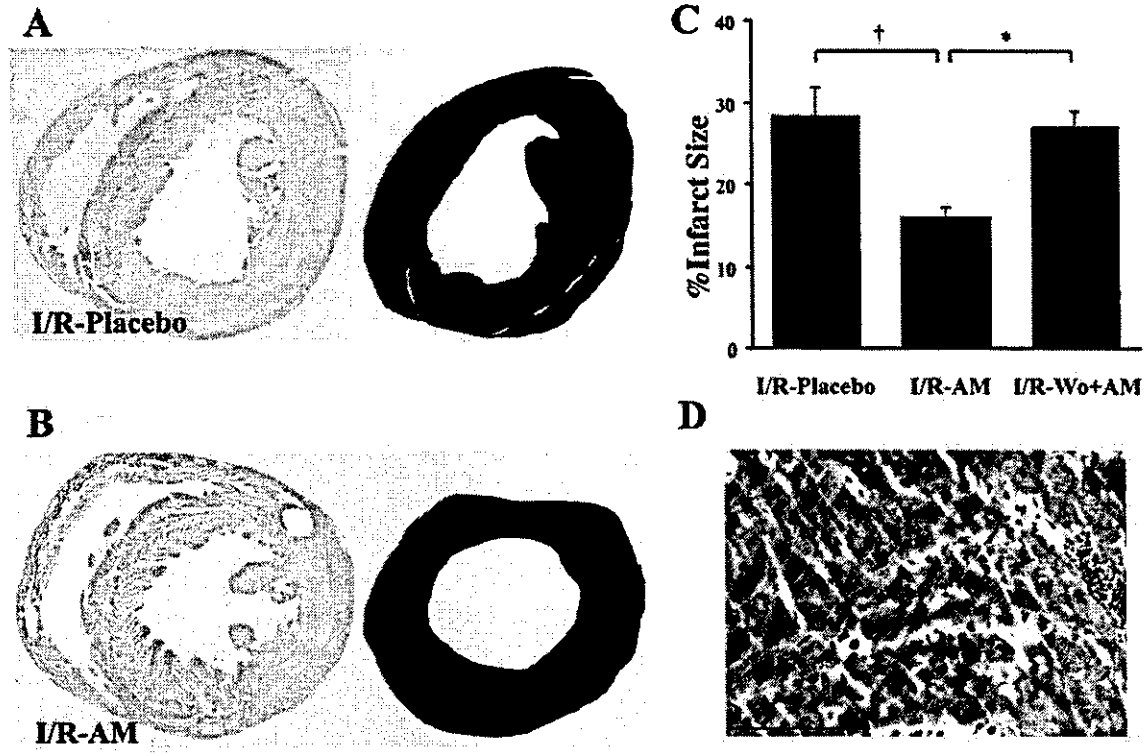

Figure 1. Effect of AM on myocardial infarct size 24 hours after ischemia/reperfusion. A and B, Photomicrographs show representative myocardial sections stained with Masson trichrome in I/R-placebo (A) and I/R-AM groups (B). Light red area indicates coagulation necrosis (right). C, Quantitative analysis demonstrated that AM infusion decreased infarct size after ischemia/reperfusion. However, pretreatment with wortmannin attenuated effect of AM. D, Typical reperfusion injury was observed in all groups on high-power field. Bar=100 μm. Data are mean±SEM. *$P<0.05$, †$P<0.01$.

mia/reperfusion (Figures 1A and 1B). Quantitative analysis revealed that 60-minute infusion of AM (0.05 $\mu g \cdot kg^{-1} \cdot min^{-1}$) significantly reduced myocardial infarct size compared with placebo infusion (16±1 versus 28±4%, $P<0.01$; Figure 1C). Infusion of AM markedly increased plasma AM level (from 10±2 fmol/mL at baseline to 96±13 fmol/mL at 60 minutes), which suggests that the plasma AM level was pharmacologically high. Pretreatment with wortmannin reversed the reducing effects of AM on myocardial infarct size (from 16±1% to 27±2%, $P<0.05$ versus I/R-AM group; Figure 1D). Although typical reperfusion injury, including contraction bands, hemorrhage, myocardial cell coagulation, and inflammatory cell infiltration, was observed after ischemia/reperfusion (Figure 1D), there were no histological differences among the 3 groups.

Hemodynamic Effects of AM

Twenty-four hours after ischemia/reperfusion, LV end-diastolic pressure (LVEDP) showed a marked elevation in the I/R-placebo group (19±2 mm Hg); the elevation was significantly attenuated in the I/R-AM group (8±2 mm Hg, $P<0.05$; Figure 2A). Pretreatment with wortmannin attenuated the reducing effects of AM on LVEDP (from 8±2 to 17±2 mm Hg, $P<0.05$ versus I/R-AM group; Figure 2A) 24 hours after ischemia/reperfusion. LV dP/dt_{max} tended to be higher in the I/R-AM group than in the I/R-placebo group (5285±285 versus 4524±247 mm Hg/s), and LV dP/dt_{min} tended to be lower in the I/R-AM group than in the I/R-placebo group (−4700±303 versus −3695±165 mm Hg/s; Figure 2B). Furthermore, pretreatment with wortmannin reversed the effects of AM on LV dP/dt_{max} and LV dP/dt_{min} after ischemia/reperfusion (5285±285 to 4570±239 mm Hg/s, −4700±303 to −3843±227 mm Hg/s, respectively; Figure 2B). These results suggest that AM infusion improved LV systolic and diastolic function after ischemia/reperfusion through the PI3K pathway. Interestingly, heart rate was significantly higher in the I/R-placebo and I/R-AM groups than in the sham group (Table). Although mean aortic pressure was significantly lower in the I/R-placebo group than in the sham group, a significant decrease in mean aortic pressure was not observed in the I/R-AM group. Right ventricular systolic pressure was significantly lower in the I/R-AM group than in the I/R-placebo group.

Antiapoptotic Effect of AM in Cardiomyocytes

Representative photomicrographs showed that TUNEL-positive myocytes were more frequently observed in the I/R-placebo group than in the sham group. However, TUNEL-positive myocytes were less frequently observed in the I/R-AM group than in the I/R-placebo group (Figure 3). Although a typical DNA ladder indicating fragmented DNA in cardiomyocytes was also observed in the I/R-placebo group, it was attenuated in the I/R-AM group (Figure 4). Quantitative analyses demonstrated that the number of TUNEL-positive cardiomyocytes was significantly smaller in the I/R-AM group than in the I/R-placebo group (9±4%

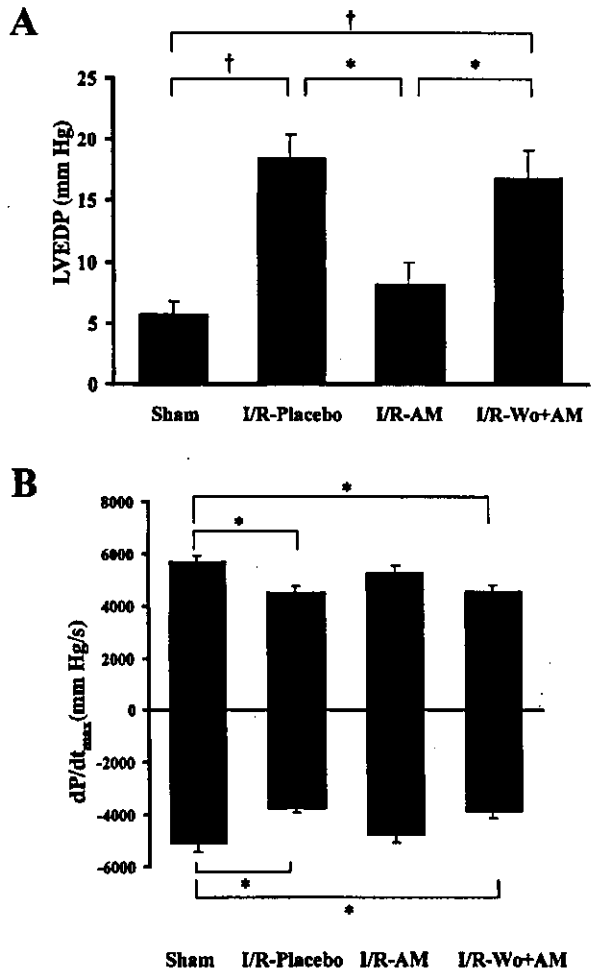

Figure 2. Effects of AM on LVEDP (A) and LV dP/dt (B) 24 hours after ischemia/reperfusion. AM infusion significantly inhibited increase in LVEDP compared with placebo infusion. AM infusion also improved LV dP/dt 24 hours after ischemia/reperfusion. Pretreatment with wortmannin attenuated effects of AM on LVEDP and LV dP/dt. Data are mean±SEM. *P<0.05; †P<0.01.

versus 19±2%, P<0.05; Figure 5). Furthermore, pretreatment with wortmannin abolished the AM-induced antiapoptotic effect in cardiomyocytes (from 9±4% to 20±1%, P<0.05; Figure 5). These results suggest that AM exerted antiapoptotic effects through the PI3K-dependent signal.

Summary of Hemodynamic Studies

	Sham (n=5)	I/R-Placebo (n=8)	I/R-AM (n=8)	I/R-Wo+AM (n=10)
Body weight, g	184±10	184±9	183±7	195±6
Heart rate, bpm	450±10	501±5*	494±9*	488±4
MAP, mm Hg	120±3	97±3*	105±4	99±7*
RAP, mm Hg	3±1	5±2	4±1	3±1
RVSP, mm Hg	32±1	47±1†	43±2†‡	48±2†

MAP indicates mean aortic pressure; RAP, right atrial pressure; and RVSP, right ventricular systolic pressure. Data are mean±SEM.

*P<0.05 vs sham group.

†P<0.01 vs Sham group.

‡P<0.01 vs I/R-placebo group.

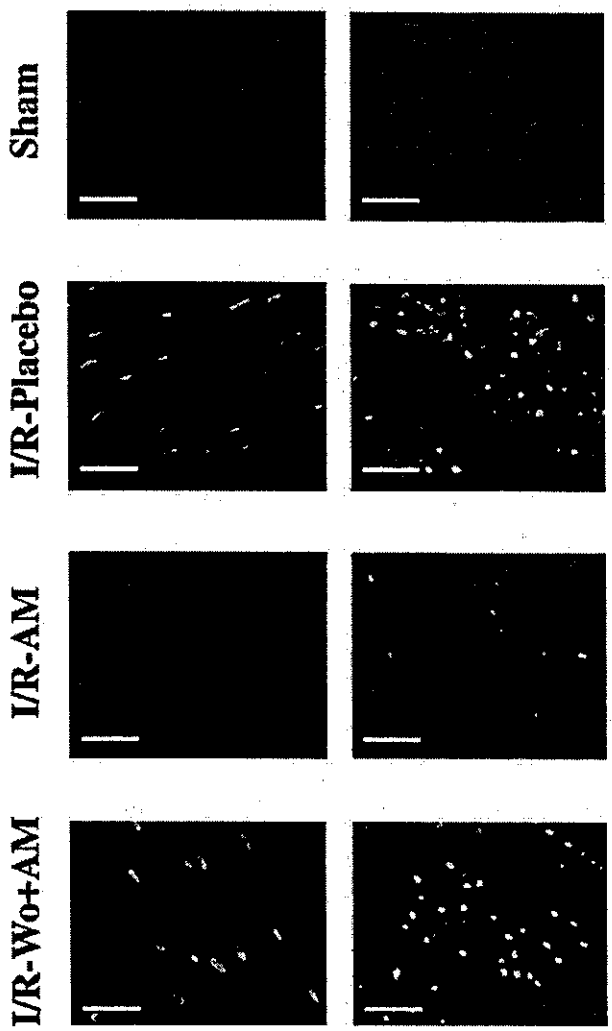

Figure 3. Representative photomicrographs of immunofluorescent staining for TUNEL-positive nuclei in sham, I/R-placebo, I/R-AM, and I/R-Wo+AM groups. Each left panel shows longitudinal myocytes, and each right panel shows short-axial myocytes. Yellow nuclei with red-stained myofilaments indicate TUNEL-positive myocytes. TUNEL-positive myocytes were less frequently observed in I/R-AM group than in I/R-placebo group. Pretreatment with wortmannin increased number of TUNEL-positive nuclei despite receipt of AM. Original magnification ×600. Bar=20 μm.

Akt Phosphorylation Induced by AM Infusion in Cardiac Tissue

Immunohistochemical analysis revealed that CRLR, a receptor for AM, was localized in cardiomyocytes and vascular endothelial cells (Figure 6). After 60-minute infusion of AM, Akt phosphorylation was detected in the nuclei of cardiomyocytes and vascular endothelial cells (Figures 7A and 7B). Western blot analyses also revealed that AM at 0.05 $\mu g \cdot kg^{-1} \cdot min^{-1}$ significantly phosphorylated Akt in cardiac tissue that was exposed to ischemia/reperfusion (Figure 7C). The effect of AM on Akt was inhibited by pretreatment with wortmannin. These results suggest that AM acts directly on myocardium and induces cardioprotective effects through the activation of PI3K/Akt-pathway.

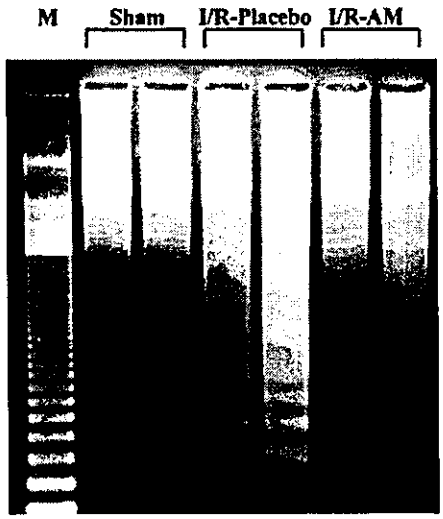

Figure 4. DNA ladder in sham, I/R-placebo, and I/R-AM groups. Although typical DNA ladder indicating fragmented DNA in cardiomyocytes was observed in I/R-placebo group, it was attenuated in I/R-AM group. M indicates molecular marker.

Discussion

In the present study, we demonstrated that short-term infusion of AM during the early phase of ischemia/reperfusion significantly reduced myocardial infarct size and inhibited myocyte apoptosis, and AM significantly decreased LVEDP and tended to improve LV dP/dt_{max} and dP/dt_{min}. We also demonstrated that AM enhanced Akt phosphorylation in cardiac tissue and that pretreatment with a PI3K inhibitor attenuated AM-induced cardioprotective effects against ischemia/reperfusion and inhibited AM-induced Akt phosphorylation.

Intravenous infusion of AM has beneficial hemodynamic and renal effects in patients with heart failure.[8] However, whether AM has direct cardioprotective effects in vivo remains unclear. In the present study, we demonstrated that short-term infusion of AM during the early phase of ischemia/reperfusion markedly reduced myocardial infarct size. Cardiomyocyte apoptosis is one of the major contributors to the development of myocardial infarcts,[15,16] which is related to the pathogenesis of heart failure. Thus, we examined whether AM has antiapoptotic effects in cardiomyocytes. Interestingly, short-term infusion of AM significantly reduced myocyte apoptosis after ischemia/reperfusion. This is the first study to demonstrate antiapoptotic effects of AM against myocardial ischemia/reperfusion injury, although AM has been shown to have antiapoptotic effects in vascular endothelial cells.[17,18] Given that cardiomyocyte apoptosis rather than necrosis contributes to myocyte death after ischemia/reperfusion, the antiapoptotic effects of AM may result in the reduced infarct size after ischemia/reperfusion.

In the present study, 60-minute infusion of AM improved cardiac function after ischemia/reperfusion, as indicated by a significant decrease in LVEDP and a tendency for an increase in LV dP/dt_{max} and a decrease in LV dP/dt_{min}. Previous studies have shown that the susceptibility to cardiac dysfunction

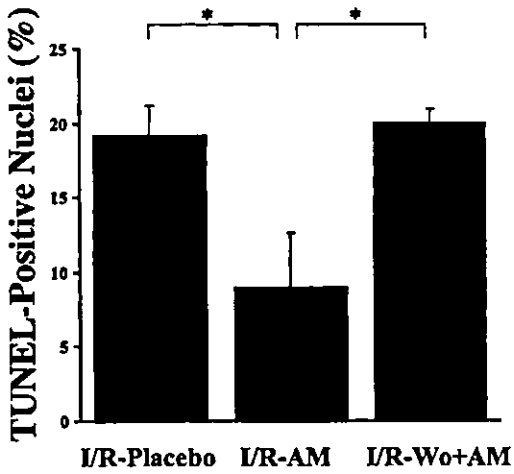

Figure 5. Quantitative analysis of TUNEL-positive nuclei in myocytes. Number of TUNEL-positive myocytes was lower in I/R-AM group than in I/R-placebo group. However, number of TUNEL-positive myocytes in I/R-Wo+AM group was as large as in I/R-placebo group. Data are mean±SEM. *$P<0.05$.

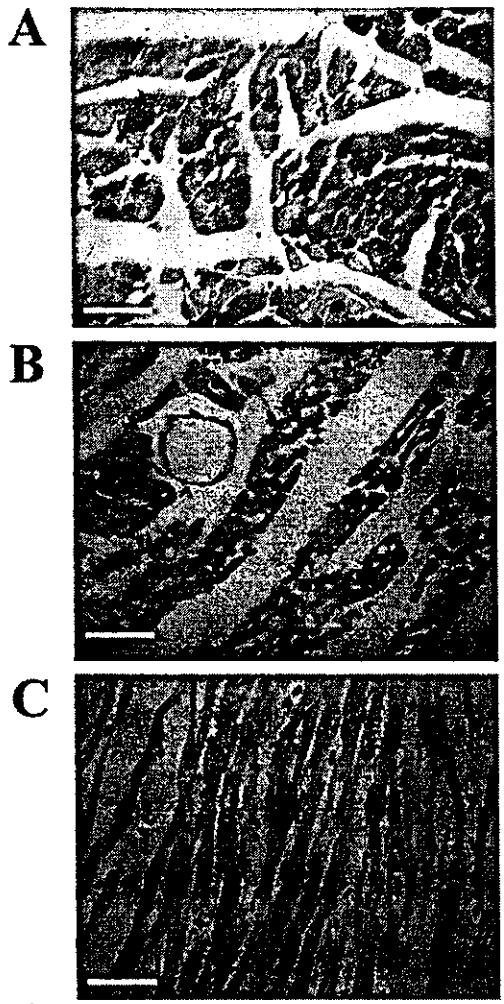

Figure 6. Immunohistochemistry for CRLR in rat cardiac tissue. Representative photomicrographs revealed that CRLR was localized in cardiomyocytes (A) and vascular endothelial cells (B). Negative control study (using mouse IgG) showed no positive staining in cardiac tissue (C). Original magnification ×400. Bar=20 μm.

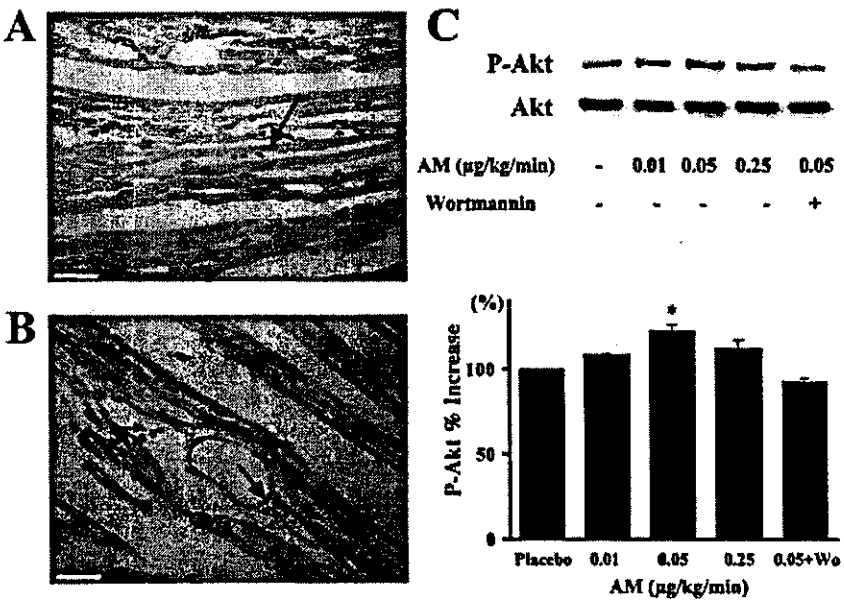

Figure 7. A and B, Immunohistochemistry for Akt phosphorylation in rat cardiac tissue. Infusion of AM (0.05 $\mu g \cdot kg^{-1} \cdot min^{-1}$) phosphorylated Akt predominantly in nuclei of cardiomyocytes (A, B) and vascular endothelial cells (B). Arrow indicates nuclei of cardiomyocytes with positive staining for P-Akt antibody. Arrowhead indicates nuclei of endothelium with positive staining for P-Akt antibody. Original magnification ×400. Bar=20 μm. C, Western blot analysis of AM-induced Akt phosphorylation in cardiac tissues. Infusion of AM (0.05 $\mu g \cdot kg^{-1} \cdot min^{-1}$) activated Akt in myocardial tissues exposed to ischemia/reperfusion. Pretreatment with wortmannin significantly inhibited AM-induced Akt phosphorylation. P-Akt indicates phosphorylated Akt; Wo, wortmannin. Data are mean±SEM. *$P<0.05$ vs placebo.

depends on the degree of myocyte apoptosis within 24 hours after ischemia/reperfusion.[19] Thus, the early prevention of myocyte apoptosis and the resultant reduced infarct size by AM may contribute to the hemodynamic improvement after ischemia/reperfusion. AM infusion reduced right ventricular systolic pressure, which may be attributable not only to the potent vasodilatory effects of AM but also to improvement in cardiac function.

Recently, Akt activation has been shown to reduce myocyte apoptosis and thereby prevent myocardial injury after transient ischemia.[10] Akt is the downstream effector molecule for signal transduction initiated by cardioprotective hormones such as insulin-like growth factor I.[20] Thus, Akt is considered to be a powerful survival signal in myocytes.[21] More recently, AM has been shown to activate the PI3K/Akt-pathway in vascular endothelial cells.[9] However, localization of AM-specific receptors in cardiac tissue had been unknown. The present study demonstrated that CRLR was present in rat cardiomyocytes and vascular endothelial cells and that AM infusion accelerated Akt phosphorylation in nuclei of cardiomyocytes and vascular endothelial cells. Furthermore, Western blot analyses demonstrated that AM 0.05 $\mu g \cdot kg^{-1} \cdot min^{-1}$ significantly increased phosphorylated Akt in cardiac tissue compared with placebo treatment and that pretreatment with wortmannin significantly inhibited Akt phosphorylation. Interestingly, pretreatment with wortmannin attenuated the AM-induced beneficial effects, such as reduction of infarct size, hemodynamic improvements, and inhibition of apoptosis. These findings suggest that AM infusion directly induces cardioprotective effects through the PI3K/Akt-dependent pathway.

In the present study, plasma AM level during infusion was much higher than baseline plasma level in rats, plasma level in normal human subjects (≈10 fmol/mL),[8] and plasma level in patients with acute myocardial infarction (≈14 fmol/mL).[22] These findings suggest that exogenously administered AM functions at pharmacological levels.

Preclinical studies have demonstrated that a variety of antioxidative or antiapoptotic agents reduce myocardial infarct size after ischemia/reperfusion.[23,24] However, few agents are clinically available for patients with coronary artery disease. In contrast, the safety and hemodynamic benefits of short-term treatment with intravenous AM (0.05 $\mu g \cdot kg^{-1} \cdot min^{-1}$) have been demonstrated in patients with heart failure[8] and patients with myocardial infarction.[25] Given the results of the present study, a prospective, randomized, placebo-controlled clinical trial should be planned.

Conclusions

Short-term infusion of AM significantly attenuated myocardial ischemia/reperfusion injury. These cardioprotective effects were attributed mainly to the antiapoptotic effects of AM via a PI3K/Akt-dependent pathway.

Acknowledgments

This work was supported in part by grants from the Ministry of Health, Labor and Welfare, the Ministry of Education, Culture, Sports, Science and Technology, the Organization for Pharmaceutical Safety and Research (OPSR) of Japan, and HLSRG H14 genome-005. We thank Kazuyoshi Masuda, Kazuhiko Akutagawa, Hiroyuki Hatsuyama, and Noriko Emoto for their pathological technical assistance and Naotaka Ota for his genetic technical assistance.

References

1. Kitamura K, Kangawa K, Kawamoto M, et al. Adrenomedullin: a novel hypotensive peptide isolated from human pheochromocytoma. *Biochem Biophys Res Commun.* 1993;192:553–560.
2. Ichiki Y, Kitamura K, Kangawa K, et al. Distribution and characterization of immunoreactive adrenomedullin in human tissue and plasma. *FEBS Lett.* 1994;338:6–10.
3. Sakata J, Shimokubo T, Kitamura K, et al. Distribution and characterization of immunoreactive rat adrenomedullin in tissue and plasma. *FEBS Lett.* 1994;352:105–108.
4. Miyao Y, Nishikimi T, Goto Y, et al. Increased plasma adrenomedullin levels in patients with acute myocardial infarction in proportion to the clinical severity. *Heart.* 1998;79:39–44.

5. Nagaya N, Nishikimi T, Yoshihara F, et al. Cardiac adrenomedullin gene expression and peptide accumulation after acute myocardial infarction in rats. *Am J Physiol Regul Integr Comp Physiol.* 2000;278:R1019–R1026.
6. Tsuruda T, Johji K, Kitamura K, et al. Adrenomedullin: a possible autocrine or paracrine inhibitor of hypertrophy of cardiomyocytes. *Hypertension.* 1998;31:505–510.
7. Tsuruda T, Johji K, Kitamura K, et al. An autocrine or a paracrine role of adrenomedullin in modulating cardiac fibroblast growth. *Cardiovasc Res.* 1999;43:958–967.
8. Nagaya N, Satoh T, Nishikimi T, et al. Hemodynamic, renal, and hormonal effects of adrenomedullin infusion in patients with congestive heart failure. *Circulation.* 2000;101:498–503.
9. Nishimatsu H, Suzuki E, Nagata D, et al. Adrenomedullin induces endothelium-dependent vasorelaxation via the phosphatidylinositol 3-kinase/Akt-dependent pathway in rat aorta. *Circ Res.* 2001;89:63–70.
10. Matsui T, Tao J, del Monte F, et al. Akt activation preserves cardiac function and prevents injury after transient cardiac ischemia in vivo. *Circulation.* 2001;104:330–335.
11. Nagaya N, Nishikimi T, Horio T, et al. Cardiovascular and renal effects of adrenomedullin in rats with heart failure. *Am J Physiol.* 1999;276:R213–R218.
12. Gao F, Gao E, Yue TL, et al. Nitric oxide mediates the antiapoptotic effect of insulin in myocardial ischemia-reperfusion: the roles of PI3-kinase, Akt, and endothelial nitric oxide synthase phosphorylation. *Circulation.* 2002;105:1497–1502.
13. Kurrelmeyer KM, Michael LH, Baumgarten G, et al. Endogenous tumor necrosis factor protects the adult cardiac myocyte against ischemic-induced apoptosis in a murine model of acute myocardial infarction. *Proc Natl Acad Sci U S A.* 2000;97:5456–5461.
14. Scarabelli TM, Knight RA, Rayment NB, et al. Quantitative assessment of cardiac myocyte apoptosis in tissue sections using the fluorescence-based TUNEL technique enhanced with counterstains. *J Immunol Methods.* 1999;228:23–28.
15. Gottlieb RA, Burleson KO, Kloner RA, et al. Reperfusion injury induces apoptosis in rabbit cardiomyocytes. *J Clin Invest.* 1994;94:1621–1628.
16. Bialik S, Geenen DL, Sasson IE, et al. Myocyte apoptosis during acute myocardial infarction in the mouse localizes to hypoxic regions but occurs independently of p53. *J Clin Invest.* 1997;100:1363–1372.
17. Kato H, Shichiri M, Marumo F, et al. Adrenomedullin as an autocrine/paracrine apoptosis survival factor for rat endothelial cells. *Endocrinology.* 1997;138:2615–2620.
18. Sata M, Kakoki M, Nagata D, et al. Adrenomedullin and nitric oxide inhibit human endothelial cell apoptosis via a cyclic GMP-independent mechanism. *Hypertension.* 2000;36:83–88.
19. Colucci WS. Apoptosis in the heart. *N Engl J Med.* 1996;335:1224–1226.
20. Yamashita K, Kajstura J, Discher DJ, et al. Reperfusion-activated Akt kinase prevent apoptosis in transgenic mouse hearts overexpressing insulin-like growth factor-1. *Circ Res.* 2001;88:609–614.
21. Franke TF, Kaplan DR, Cantley LC, et al. PI3K: downstream AKTion blocks apoptosis. *Cell.* 1997;88:435–437.
22. Miyao Y, Nishikimi T, Goto Y, et al. Increased plasma adrenomedullin levels in patients with acute myocardial infarction in proportion to the clinical severity. *Heart.* 1998;79:39–44.
23. Yaoita H, Ogawa K, Maehara K, et al. Attenuation of ischemia/reperfusion injury in rats by caspase inhibitor. *Circulation.* 1998;97:276–281.
24. Wang P, Chen H, Qin H, et al. Overexpression of human copper, zinc-superoxide dismutase (SOD1) prevents postischemic injury. *Proc Natl Acad Sci U S A.* 1998;95:4556–4560.
25. Nagaya N, Goto Y, Satoh T, et al. Intravenous adrenomedullin in myocardial function and energy metabolism in patients after myocardial infarction. *J Cardiovasc Pharmacol.* 2002;39:754–760.

Adrenomedullin Gene Transfer Induces Therapeutic Angiogenesis in a Rabbit Model of Chronic Hind Limb Ischemia

Benefits of a Novel Nonviral Vector, Gelatin

Noriyuki Tokunaga, MD; Noritoshi Nagaya, MD; Mikiyasu Shirai, MD; Etsuro Tanaka, MD; Hatsue Ishibashi-Ueda, MD; Mariko Harada-Shiba, MD; Munetake Kanda, MD; Takefumi Ito, MD; Wataru Shimizu, MD; Yasuhiko Tabata, PhD; Masaaki Uematsu, MD; Kazuhiro Nishigami, MD; Shunji Sano, MD; Kenji Kangawa, PhD; Hidezo Mori, MD

Background—Earlier studies have shown that adrenomedullin (AM), a potent vasodilator peptide, has a variety of cardiovascular effects. However, whether AM has angiogenic potential remains unknown. This study investigated whether AM gene transfer induces therapeutic angiogenesis in chronic hind limb ischemia.

Methods and Results—Ischemia was induced in the hind limb of 21 Japanese White rabbits. Positively charged biodegradable gelatin was used to produce ionically linked DNA-gelatin complexes that could delay DNA degradation. Human AM DNA (naked AM group), AM DNA-gelatin complex (AM-gelatin group), or gelatin alone (control group) was injected into the ischemic thigh muscles. Four weeks after gene transfer, significant improvements in collateral formation and hind limb perfusion were observed in the naked AM group and AM-gelatin group compared with the control group (calf blood pressure ratio: 0.60 ± 0.02, 0.72 ± 0.03, 0.42 ± 0.06, respectively). Interestingly, hind limb perfusion and capillary density of ischemic muscles were highest in the AM-gelatin group, which revealed the highest content of AM in the muscles among the three groups. As a result, necrosis of lower hind limb and thigh muscles was minimal in the AM-gelatin group.

Conclusions—AM gene transfer induced therapeutic angiogenesis in a rabbit model of chronic hind limb ischemia. Furthermore, the use of biodegradable gelatin as a nonviral vector augmented AM expression and thereby enhanced the therapeutic effects of AM gene transfer. Thus, gelatin-mediated AM gene transfer may be a new therapeutic strategy for the treatment of peripheral vascular diseases. (***Circulation.*** **2004;109:526-531.)**

Key Words: peripheral vascular disease ■ angiogenesis ■ gene therapy ■ ischemia

Adrenomedullin (AM) is a potent vasodilator peptide that was originally isolated from human pheochromocytoma.[1] AM and its receptor are expressed mainly in vascular endothelial cells and vascular smooth muscle cells.[2–4] AM not only induces vasorelaxation but also regulates growth and death of these vascular cells.[5–10] These findings suggest that AM plays an important role in maintaining vascular homeostasis in an autocrine and/or paracrine manner.

A recent study has shown that vascular abnormalities are present in homozygous AM knockout mice, suggesting that AM is indispensable for vascular morphogenesis.[11–13] More recently, AM has been shown to activate the PI3K/Akt-dependent pathway in vascular endothelial cells, which is considered to regulate multiple critical steps in angiogenesis, including endothelial cell survival, proliferation, migration, and capillary-like structure formation.[7,14] These results raise the possibility that AM plays a role in modulating vasculogenesis and angiogenesis. However, whether AM induces therapeutic angiogenesis remains unknown.

Received May 20, 2003; revision received September 25, 2003; accepted September 26, 2003.

From the Department of Cardiac Physiology, National Cardiovascular Center Research Institute, Osaka, Japan (N.T., M.S., M.K., H.M.); the Department of Cardiovascular Surgery, Okayama University Medical School, Okayama, Japan (N.T., S.S.); the Department of Regenerative Medicine and Tissue Engineering, National Cardiovascular Center Research Institute, Osaka, Japan (N.N., T.I.); the Department of Internal Medicine, National Cardiovascular Center, Osaka, Japan (N.N., W.S., K.N.); the Department of Physiology, the Research Center for Genetic Engineering and Cell Transplantation, Tokai University School of Medicine, Isehara, Japan (E.T.); the Department of Pathology, National Cardiovascular Center, Osaka, Japan (H.I.-U.); the Department of Biochemistry, National Cardiovascular Center Research Institute, Osaka, Japan (M.H.-S., K.K.); the Department of Biomaterials, Field of Tissue Engineering, Institute for Frontier Medical Sciences, Kyoto University, Kyoto, Japan (Y.T.); and the Cardiovascular Division, Kansai Rosai Hospital, Hyogo, Japan (M.U.).

Correspondence to Noritoshi Nagaya, MD, Department of Regenerative Medicine and Tissue Engineering or Hidezo Mori, MD, Department of Cardiac Physiology, National Cardiovascular Center Research Institute, 5-7-1 Fujishirodai, Suita, Osaka 565-8565, Japan. E-mail nagayann@hsp.ncvc.go.jp or hidemori@ri.ncvc.go.jp

Circulation is available at http://www.circulationaha.org

DOI: 10.1161/01.CIR.0000109700.81266.32

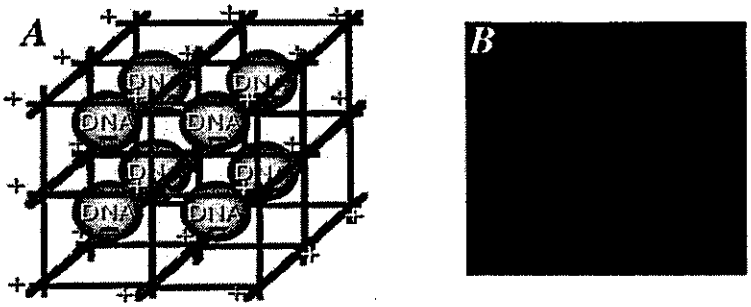

Figure 1. A, Schema of DNA-gelatin complex. Biodegradable gelatin can hold negatively charged plasmid DNA in its positively charged lattice structure. B, RITC-labeled AM DNA particles were incorporated into gelatin.

We prepared biodegradable gelatin that could hold negatively charged protein or plasmid DNA in its positively charged lattice structure.[15,16] Biodegradable gelatin has been widely used as a carrier of protein because of its capacity to delay protein degradation.[15] Similarly, ionically linked DNA-gelatin complexes can delay gene degradation.[16] These findings raise the possibility that gelatin may serve as a nonviral vector for gene therapy.

Thus, the purposes of this study were (1) to investigate whether AM gene transfer induces therapeutic angiogenesis in a rabbit model of chronic hind limb ischemia and (2) to examine whether the use of biodegradable gelatin as a vector augments AM expression and thereby enhances the therapeutic effects of AM gene transfer.

Methods

Animal Model

All protocols were performed in accordance with the guidelines of the Animal Care Ethics Committee of the National Cardiovascular Center Research Institute. Twenty-one male Japanese White rabbits (body weight, 2.9±0.1 kg; Japan Animal Co, Osaka, Japan) were used for physiological and morphological assessment. In addition, 30 rabbits were used for radioimmunoassay, immunohistochemical examination, and Western blot analysis. After anesthetization with pentobarbital sodium (30 to 35 mg/kg), a longitudinal incision was made in the left thigh, extending inferiorly from the inguinal ligament to a point just proximal to the patella. Hind limb ischemia was induced by ligation of the distal left external iliac artery and complete resection of the left femoral artery, as described previously.[17]

Construction of Plasmid DNA

To construct the expression vector for human AM, the *EcoRI/XhoI* fragment of the full-length human AM cDNA was ligated into the EcoRI/XhoI fragment of the pcDNA1.1-CMV expression plasmid (Invitrogen). To verify that the pcDNA1.1-CMV vector encoding AM cDNA produces a biologically active AM protein, the expression vector was transfected into 293 cells, and AM activity in the transfected cells was measured by high-performance liquid chromatography and radioimmunoassay. The pcDNA1.1-CMV vector encoding β-galactosidase (LacZ) cDNA was used as a control DNA.

Preparation of AM DNA-Gelatin Complex

Biodegradable gelatin was prepared from pig skin. The gelatin was characterized by a spheroid shape with a diameter of approximately 30 μm, water content of 95%, and an isoelectric point (pI) of 9 after swelling in water.[15,16] Gelatin can hold negatively charged protein or plasmid DNA in its positively charged lattice structure (Figure 1A). Dried gelatin (4 mg, pI 9) was added to human AM DNA solution (500 μg/100 μL in phosphate-buffered saline, pH 7.4). After mixture of DNA and gelatin, DNA-gelatin complexes were incubated at 37°C for 2 hours.

To visualize incorporation of DNA into gelatin, AM plasmid DNA was labeled with rhodamine B isothiocyanate (RITC), as reported previously.[16] In brief, the coupling reaction of RITC to plasmid DNA was carried out by mixing the two substances in 0.2 mol/L sodium carbonate-buffered solution (pH 9.7), followed by gel filtration with a PD 10 column (Amersham-Pharmacia). RITC-labeled AM DNA was incorporated into positively charged gelatin (Figure 1B).

Study Protocol

Ten days after the induction of hind limb ischemia (day 10), AM DNA (naked AM group, n=7), AM DNA-gelatin complex (AM-gelatin group, n=7), or gelatin alone (control group, n=7) was administered intramuscularly into 3 different sites in the ischemic adductor muscle and 2 different sites in the semimembranous muscle. In addition, Lac Z DNA-gelatin complex served as a control DNA (Lac Z-gelatin group, n=5). The amount of plasmid was 500 μg (1 mL) and that of gelatin was 4 mg. Morphological and angiographic analyses and measurements of calf blood pressure and laser Doppler flow were performed 4 weeks after gene transfer (day 38). After completion of these measurements, the adductor, semimembranous, and gastrocnemius muscles were weighed in each hind limb.[18] The muscle weight ratio was calculated for each muscle as follows: muscle weight ratio=muscle weight in ischemic hind limb/muscle weight in nonischemic hind limb. Specimens of the adductor muscle of the ischemic hind limb were obtained for histological examination.

Measurement of Calf Blood Pressure

Calf blood pressure was measured on days 10 and 38 in both hind limbs with a Doppler flowmeter (Hayashi Denki Co, Ltd) and a 25-mm-wide cuff. The pulse of the posterior tibial artery was identified with the use of a Doppler probe, and the systolic blood pressure in both hind limbs was determined by standard techniques. The calf blood pressure ratio was defined for each rabbit as the ratio of systolic pressure of the ischemic hind limb to that of the normal hind limb.[17]

Laser Doppler Blood Perfusion Analysis

Blood flow of the ischemic hind limb was measured with the use of a laser Doppler blood perfusion image system (moorLDI, Moor Instruments) on day 38.

Angiographic Analysis

Development of collateral arteries was evaluated by angiography on days 0 and 38. A 4F catheter was placed in the left internal iliac artery through the common carotid artery, and 3 mL contrast medium (Iopamiron 300, SCHERING) was injected with an automated angiography injector at a rate of 2.5 mL/s. Quantitative angiographic analysis of collateral vessel development in the ischemic hind limb was performed with the use of a 5-mm^2 grid overlay, as described previously.[17] The angiographic score was calculated for each film as the ratio of grid intersections crossed by opacified arteries divided by the total number of grid intersections in the ischemic medial thigh. The angiographic score was determined by 2 blinded observers.

Morphological and Histological Examination

The degree of lower hind limb necrosis and thigh muscle necrosis was macroscopically evaluated on graded morphological scales (grade 1 to 3) for peripheral tissue damage and muscle necrosis area of the adductor, semimembranous, and medial large muscles. Capillary density of the ischemic hind limb was evaluated by alkaline phosphatase staining, as reported previously.[17] A total of 10 different fields from three different sections were randomly selected, and the number of capillaries was counted under a ×40 objective. Capillary density was expressed as the mean number of capillaries per square millimeter. The number of myofibers in each field was also examined and the capillary/muscle fiber ratio calculated.

Radioimmunoassay for Human AM

Human AM production was examined 1, 2, and 4 weeks after gene transfer in the naked AM group, AM-gelatin group, and control group (n=5 each). The muscles were harvested for radioimmunoassay and immunohistochemical examination. Immunoreactive human AM level in rabbit muscles was determined by immunoradiometric assay with the use of a specific kit (Shionogi Co, Ltd).[19] Tissue content of vascular endothelial growth factor (VEGF) was examined by ELISA kit (R&D systems).

Immunohistochemistry for Human AM, Ki67 Antigen, and Phosphorylated Akt

Immunohistochemical studies were performed on formalin-fixed, paraffin-embedded 4-μm sections of ischemic thigh muscles 7 days after gene transfer. To elucidate AM expression after gene therapy, immunohistochemistry for human AM was performed with the use of a monoclonal antibody recognizing AM-(12–25) (1:100), as reported previously.[20] To evaluate the proliferative potential of AM, tissue sections were stained for Ki67, a marker for cell proliferation, with the use of monoclonal anti-Ki67 antibody (1:100) (DAKO). AM has recently been shown to promote proliferation of vascular endothelial cells at least in part through the PI3k/Akt pathway.[21] Thus, immunohistochemistry for phosphorylated Akt was performed with mouse monoclonal anti-phosphorylated Akt antibody (1:100) (Cell Signaling Technology).

Western Blot Analysis

To identify Akt phosphorylation in ischemic muscles after AM gene transfer, Western blotting was performed with the use of a commercially available kit (PhosphoPlus Akt [Ser473] Antibody Kit, Cell Signaling Technology). Ischemic muscles in the 3 groups were obtained 7 days after AM gene transfer. These samples were homogenized on ice in 0.1% Tween 20 homogenization buffer with a protease inhibitor (Complete, Roche). After centrifugation for 20 minutes at 4°C, the supernatant was used for Western blot analysis. The 50 μg of protein was transferred into sample buffer, loaded on 7.5% SDS-polyacrylamide gel, and blotted onto nitrocellulose membrane through the use of a wet blotting system. After blocking for 60 minutes, the membranes were incubated with primary antibodies (1:500) at 4°C overnight. The membranes were then incubated with secondary antibodies, which were conjugated with horseradish peroxidase (Cell Signaling Technology), at a final dilution of 1:2000. Signals were detected through the use of LumiGLO chemiluminescence reagents (Cell Signaling Technology).

Statistical Analysis

All results are expressed as mean±SEM. Statistical significance was evaluated by 1-way ANOVA followed by Fisher's analysis, Scheffe's F analysis, or Kruskal-Wallis test. A value of $P<0.05$ was considered statistically significant.

Results

Physiological and Morphological Assessment

Complete resection of the left femoral artery resulted in a similar decrease in calf blood pressure ratio among the 3 groups before the initiation of therapy (day 10) (Figure 2A). However, the calf blood pressure ratio on day 38 was highest in the AM-gelatin groups, followed by the naked AM group and subsequently the control group. The laser Doppler flow in hind limb was highest in the AM-gelatin group, followed by the naked AM group and the control group (Figure 2B). The calf blood pressure ratio and laser Doppler flow 4 weeks after gene transfer did not significantly differ between the control group and Lac Z-gelatin group. Lower hind limb necrosis was minimal in the AM-gelatin group, followed by the naked AM group and the control group (Figure 2C). Thigh muscle necrosis was also minimal in the AM-gelatin group. Similarly, the muscle weight ratio (ischemic/normal) on day 38 was highest in the AM-gelatin group (Table). Neither mean arterial pressure nor heart rate significantly differed among the 3 groups.

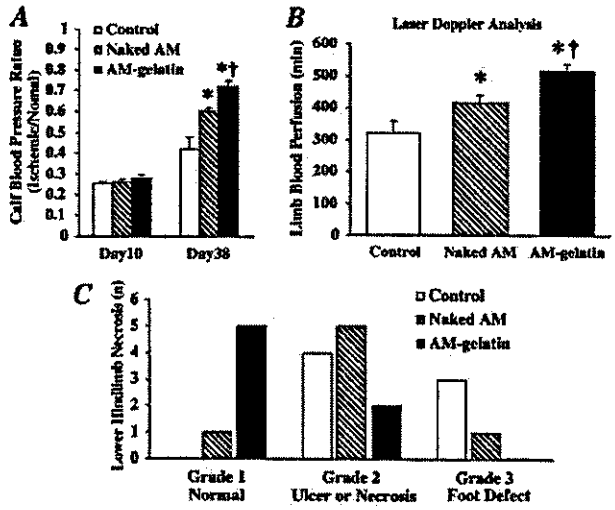

Figure 2. A, Calf blood pressure ratio (ischemic/normal hind limb) before (on day 10) and after (on day 38) gene transfer. B, Measurement of laser Doppler flow on day 38. Data are mean±SEM. *$P<0.05$ vs control group; †$P<0.05$ vs naked AM group. C, Number of cases of each grade of lower hind limb necrosis on day 38. Lower hind limb necrosis was minimal in the AM-gelatin group. Number of necrosis or foot defect is statistically significant among the 3 groups ($P<0.05$ by Kruskal-Wallis test).

Angiographic Analysis

Angiograms 4 weeks after gene transfer (day 38) showed the development of collateral arteries in the naked AM and

Physiological Characteristics

	Control	Naked AM	AM-Gelatin
No. of rabbits	7	7	7
Body weight, kg	2.46±0.06	2.65±0.10	3.16±0.09
MAP, mm Hg	112±3	114±3	116±2
HR, beats/min	269±12	253±5	262±7
Muscle weight ratio	0.71±0.03	0.84±0.02*	0.95±0.02*†

MAP indicates mean arterial pressure; HR, heart rate; and muscle weight ratio, ratio of muscle weight in ischemic hind limb to that in nonischemic hind limb. Data are mean±SEM.

*$P<0.01$ vs control group; †$P<0.05$ vs naked AM group.

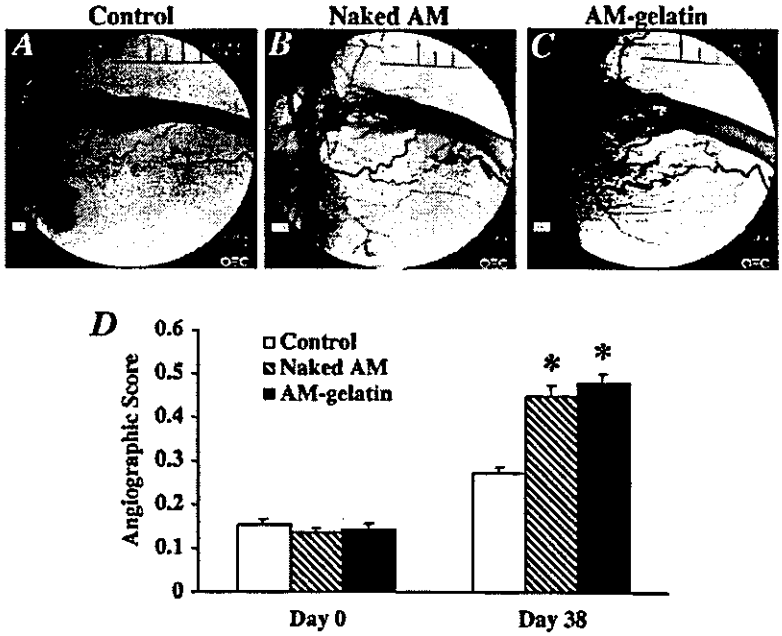

Figure 3. Representative angiograms of control group (A), naked AM group (B), and AM-gelatin group (C) on day 38. Collateral arteries were well developed in the naked AM and AM-gelatin groups. D, Angiographic score on days 0 and 38 in each group. Angiographic score on day 38 was significantly higher in the naked AM and AM-gelatin groups than in the control group. Data are mean±SEM. *$P<0.001$ versus control group.

AM-gelatin groups compared with that in the control group (Figure 3, A through C). Quantitative analysis of collateral vessels demonstrated that the angiographic score in both the naked AM and AM-gelatin groups was significantly higher than that in the control group (Figure 3D). Angiographic score did not significantly differ between the control group and Lac Z-gelatin group.

To examine the development of collateral vessels in an earlier stage, other rabbits (n=4 each) were examined 2 weeks after gene transfer (day 24). Angiograms showed significant collateral development in the naked AM and AM-gelatin groups compared with that in the control group.

Histological Examination

Alkaline phosphatase staining of ischemic hind limb muscle showed marked augmentation of neovascularization in both the naked AM and AM-gelatin groups compared with the control group (Figure 4, A through C). Quantitative analysis demonstrated that capillary density of the ischemic adductor muscle was highest in the AM-gelatin group (Figure 4D). Analysis of the capillary/muscle fiber ratio yielded similar results. Seven days after gene transfer, intense immunostaining for Ki67 was observed in vascular endothelial cells of the naked AM and the AM-gelatin groups (Figure 4, E through G).

AM Expression and Akt Phosphorylation After Gene Transfer

Seven days after gene transfer, modest immunostaining for human AM was observed in the naked AM group, whereas AM immunoreactivity was intense surrounding the gelatin in the AM-gelatin group (Figure 5, A through C). Tissue content of human AM was significantly increased both in the naked AM and the AM-gelatin groups 7 days after gene transfer (Figure 5D). The AM level in the AM-gelatin group was significantly higher that in the naked AM group. Two weeks after gene transfer, AM overexpression was observed only in the AM-gelatin group. The expression of endogenous VEGF and its receptors (Flt-1 and Flk-1) did not differ among the 3 groups (data not shown). Western blot analysis revealed that phosphorylated Akt in ischemic muscles was increased in both the naked AM and AM-gelatin groups 7 days after gene transfer (Figure 5E). Intense immunostaining for phosphory-

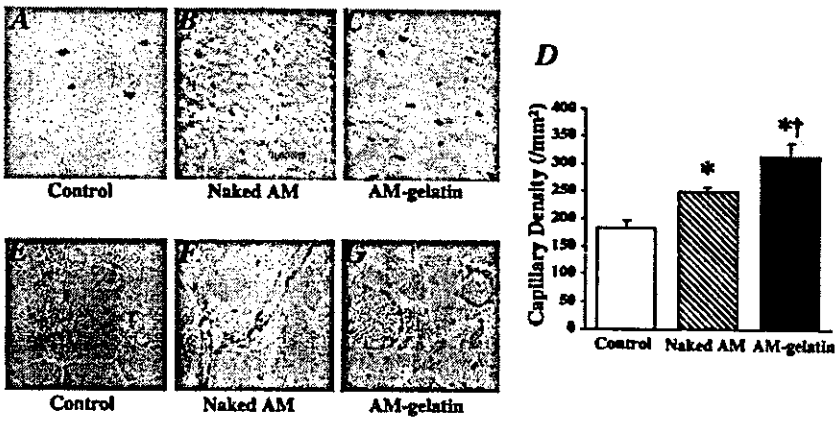

Figure 4. A through C, Representative examples of alkaline phosphatase staining in ischemic hind limb muscles. Magnification ×200. D, Quantitative analysis of capillary density in ischemic hind limb muscles. Data are mean±SEM. *$P<0.05$ vs control group; †$P<0.05$ vs naked AM group. E through G, Immunohistochemical analysis of Ki67 antigen, a marker for cell proliferation. Magnification ×400.

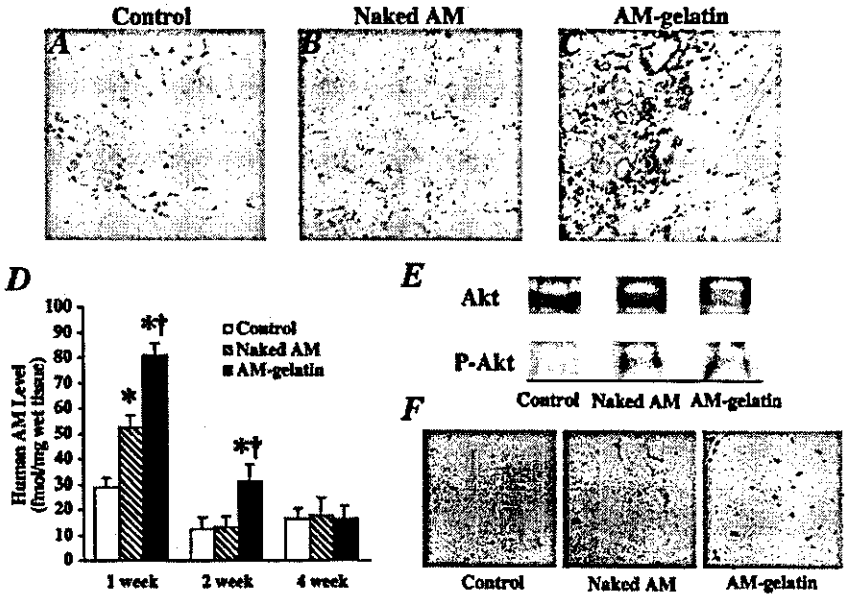

Figure 5. A through C, Immunohistochemistry for human AM 7 days after gene transfer. Intense immunostaining was observed surrounding gelatin in the AM-gelatin group. Magnification ×200. D, Time course of AM production in ischemic muscles after gene transfer. Data are mean±SEM. *$P<0.01$ vs control group; †$P<0.01$ vs naked AM group. E, Western blot analysis for Akt phosphorylation in muscles. F, Immunohistochemical staining for phosphorylated Akt 7 days after gene transfer. Phosphorylated Akt was distributed at least in endothelial cells. Magnification ×400.

lated Akt was observed at least in endothelial cells of the Naked AM and the AM-gelatin groups (Figure 5F).

Discussion

We demonstrated that (1) AM gene transfer induced hemodynamic and angiographic improvements in association with an increase in capillary density in a rabbit model of chronic hind limb ischemia. We also demonstrated that (2) administration of AM DNA-gelatin complexes markedly augmented AM expression and thereby enhanced the therapeutic effects of AM gene transfer.

AM has a variety of effects on the vasculature that include vasodilation,[1,5–7] inhibition of endothelial cell apoptosis,[8,9] and regulation of smooth muscle cell proliferation.[10] However, whether AM has angiogenic potential has remained unknown. In the present study, intramuscular administration of naked AM DNA augmented AM production in skeletal muscles, as indicated by increased tissue content and significant immunostaining of AM. As a result, AM gene transfer increased hind limb perfusion and ameliorated lower hind limb and thigh muscle necrosis in a rabbit model of hind limb ischemia. AM gene transfer may protect the ischemic hind limb partly by improving the blood flow in the ischemic hind limb because AM is originally identified as a potent vasodilating peptide.[1] Nevertheless, angiographic collateral development and high capillary density were observed in ischemic muscles after AM gene transfer. Ki67, a marker for cell proliferation, was detected in endothelial cells of microvessels after AM gene transfer. These results suggest that AM overproduction resulting from gene transfer may induce angiogenesis in a rabbit model of hind limb ischemia. Recent studies using AM gene knockout mice have shown that AM is essential for development of the vasculature during embryogenesis.[11–13] These studies support our results that AM may be an angiogenic factor. VEGF is known to induce angiogenesis and to regulate endothelial cell survival through the phosphatidylinositol 3-kinase (PI3K)/Akt pathway.[22] Thus, the PI3K/Akt pathway is considered to regulate multiple critical steps in angiogenesis, including endothelial cell survival, proliferation, migration, and capillary-like structure formation.[14] A recent study has reported that AM promotes proliferation and migration of human umbilical vein endothelial cells at least in part through the PI3K/Akt pathway.[21] The present study demonstrated that phosphorylated Akt is increased at least in endothelial cells after AM gene transfer. AM gene transfer did not influence endogenous VEGF and its receptors. Taken together, it is interesting to speculate that AM may directly induce angiogenesis through the PI3K/Akt pathway.

In the present study, we used positively charged biodegradable gelatin as a nonviral vector. We have shown that basic fibroblast growth factor (bFGF) is ionically linked with gelatin, which enhances the angiogenic effects of bFGF by delaying protein degradation.[15] Thus, biodegradable gelatin has been used as a carrier of protein. However, little information is available regarding the therapeutic potential of gelatin as a nonviral vector for gene transfer. In the present study, we demonstrated that RITC-labeled AM DNA was incorporated into positively charged gelatin. In addition, intramuscular administration of AM DNA-gelatin complexes strongly enhanced AM production compared with that of naked AM DNA. These results suggest that biodegradable gelatin may serve as a vector for gene transfer. In fact, AM DNA-gelatin complexes induced more potent angiogenic effects in a rabbit model of hind limb ischemia than naked AM DNA, as evidenced by significant increases in histological capillary density, calf blood pressure ratio, laser Doppler flow, and muscle weight ratio and a decrease in necrosis of lower hind limb and thigh muscles. These results suggest that the use of biodegradable gelatin as a nonviral vector augments AM expression and enhances AM-induced angiogenic effects. The angiogenic effects of AM-gelatin complexes were comparable to those of bFGF-gelatin complexes (data not shown). AM DNA-gelatin complexes were distributed mainly in connective tissues. We have recently demonstrated that gelatin-DNA complex is readily phagocytosed by mac-

rophages, monocytes, endothelial progenitor cells, and so on, resulting in gene expression within these phagocytes.[23,24] These findings raise the possibility that AM secreted from these cells acts on muscles in a paracrine fashion. Unlike AM production in the naked AM group, AM overexpression in the AM-gelatin group lasted for longer than 2 weeks. Thus, it is interesting to speculate that delaying gene degradation by gelatin may be responsible for the highly efficient gene transfer.

Currently, a highly efficient and safe gene delivery system is needed for gene therapy in humans. The present study demonstrated that the use of gelatin, which is considered to be less biohazardous than viral vectors, enhanced the angiogenic potential of AM DNA. Thus, gelatin-mediated AM gene transfer may be a new therapeutic strategy for the treatment of severe peripheral vascular diseases. However, the initial success of gelatin-mediated AM gene therapy reported here should be confirmed by long-term experiments, and extensive toxicity studies in animals are needed before clinical trials.

Study Limitation

First, histological capillary density, calf blood pressure ratio, and laser Doppler flow were significantly higher in the AM-gelatin group than in the naked AM group. However, the angiographic score did not significantly differ between the two. This discrepancy raises the possibility that conventional angiography may have insufficient resolution to fully visualize the angiogenic microvessels. Second, human AM level was slightly elevated in the control group. This implies that the anti-human AM antibody used in this radioimmunoassay had some cross-reactivity with endogenous rabbit AM. Nevertheless, human AM level in the muscles was highest in the AM-gelatin group within 2 weeks after gene transfer. These results suggest that AM DNA-gelatin complexes induces potent and long-lasting AM production.

Conclusions

Intramuscular administration of AM DNA induced therapeutic angiogenesis in a rabbit model of chronic hind limb ischemia. Furthermore, the use of biodegradable gelatin as a nonviral vector augmented AM expression and thereby enhanced the therapeutic effects of AM gene transfer. Thus, gelatin-mediated AM gene transfer may be a new therapeutic strategy for the treatment of peripheral vascular diseases.

Acknowledgments

This work was supported by a grant from the Japan Cardiovascular Research Foundation, HLSRG-RAMT-nano-001 and -RHGTEFB-genome-005, RGCD13C-1 from MHLW, grants from NEDO, a Grant-in-Aid for Scientific research from MECSST (13470154 and13877114), and the Promotion of Fundamental Studies in Health Science of the Organization for Pharmaceutical Safety and Research (OPSR) of Japan.

References

1. Kitamura K, Kangawa K, Kawamoto M, et al. Adrenomedullin: a novel hypotensive peptide isolated from human pheochromocytoma. *Biochem Biophys Res Commun.* 1993;192:553–560.
2. Sugo S, Minamino N, Kangawa K, et al. Endothelial cells actively synthesize and secrete adrenomedullin. *Biochem Biophys Res Commun.* 1994;201:1160–1166.
3. Sugo S, Minamino N, Shoji H, et al. Production and secretion of adrenomedullin from vascular smooth muscle cells: augmented production by tumor necrosis factor-alpha. *Biochem Biophys Res Commun.* 1994;203:719–726.
4. Kato J, Kitamura K, Kangawa K, et al. Receptors for adrenomedullin in human vascular endothelial cells. *Eur J Pharmacol.* 1995;289:383–385.
5. Shimekake Y, Nagata K, Ohta S, et al. Adrenomedullin stimulates two signal transduction pathways, cAMP accumulation and Ca^{2+} mobilization, in bovine aortic endothelial cells. *J Biol Chem.* 1995;270:4412–4417.
6. Nagaya N, Satoh T, Nishikimi T, et al. Hemodynamic, renal, and hormonal effects of adrenomedullin infusion in patients with congestive heart failure. *Circulation.* 2000;101:498–503.
7. Nishimatsu H, Suzuki E, Nagata D, et al. Adrenomedullin induces endothelium-dependent vasorelaxation via the phosphatidylinositol 3-kinase/Akt-dependent pathway in rat aorta. *Circ Res.* 2001;89:63–70.
8. Kato H, Shichiri M, Marumo F, et al. Adrenomedullin as an autocrine/paracrine apoptosis survival factor for rat endothelial cells. *Endocrinology.* 1997;138:2615–2620.
9. Sata M, Kakoki M, Nagata D, et al. Adrenomedullin and nitric oxide inhibit human endothelial cell apoptosis via a cyclic GMP-independent mechanism. *Hypertension.* 2000;36:83–88.
10. Kano H, Kohno M, Yasunari K, et al. Adrenomedullin as a novel antiproliferative factor of vascular smooth muscle cells. *J Hypertens.* 1996;14:209–213.
11. Shindo T, Kurihara Y, Nishimatsu H, et al. Vascular abnormalities and elevated blood pressure in mice lacking adrenomedullin gene. *Circulation.* 2001;104:1964–1971.
12. Caron KM, Smithies O. Extreme hydrops fetalis and cardiovascular abnormalities in mice lacking a functional adrenomedullin gene. *Proc Natl Acad Sci U S A.* 2001;98:615–619.
13. Imai Y, Shindo T, Maemura K, et al. Evidence for the physiological and pathological roles of adrenomedullin from genetic engineering in mice. *Ann N Y Acad Sci.* 2001;947:26–34.
14. Shiojima I, Walsh K. Role of Akt signaling in vascular homeostasis and angiogenesis. *Circ Res.* 2002;90:1243–1250.
15. Tabata Y, Hijikata S, Muniruzzaman M, et al. Neovascularization effect of biodegradable gelatin microspheres incorporating basic fibroblast growth factor. *J Biomater Sci Polym Ed.* 1999;10:79–94.
16. Fukunaka Y, Iwanaga K, Morimoto K, et al. Controlled release of plasmid DNA from cationized gelatin hydrogels based on hydrogel degradation. *J Control Release.* 2002;80:333–343.
17. Takeshita S, Zheng LP, Brogi E, et al. Therapeutic angiogenesis: a single intraarterial bolus of vascular endothelial growth factor augments revascularization in a rabbit ischemic hindlimb model. *J Clin Invest.* 1994;93:662–670.
18. Van Belle E, Witzenbichler B, Chen D, et al. Potentiated angiogenic effect of scatter factor/hepatocyte growth factor via induction of vascular endothelial growth factor. *Circulation.* 1998;97:381–390.
19. Ohta H, Tsuji T, Asai S, et al. A simple immunoradiometric assay for measuring the entire molecules of adrenomedullin in human plasma. *Clin Chim Acta.* 1999;287:B131–B143.
20. Nagaya N, Nishikimi T, Yoshihara F, et al. Cardiac adrenomedullin gene expression and peptide accumulation after acute myocardial infarction in rats. *Am J Physiol Regul Integr Comp Physiol.* 2000;278:R1019–R1026.
21. Miyashita K, Itoh H, Sawada N, et al. Adrenomedullin promotes proliferation and migration of cultured endothelial cells. *Hypertens Res.* 2003;26:S93–S98.
22. Jiang BH, Zheng JZ, Aoki M, et al. Phosphatidylinositol 3-kinase signaling mediates angiogenesis and expression of vascular endothelial growth factor in endothelial cells. *Proc Natl Acad Sci U S A.* 2000;97:1749–1753.
23. Tabata Y, Ikada Y. Macrophage activation through phagocytosis of muramyl dipeptide encapsulated in gelatin microspheres. *J Pharm Pharmacol.* 1987;39:698–704.
24. Nagaya N, Kangawa K, Kanda M, et al. Hybrid cell-gene therapy for pulmonary hypertension based on phagocytosing action of endothelial progenitor cells. *Circulation.* 2003;108:889–895.

0013-7227/03/$15.00/0
Printed in U.S.A.

Endocrinology 144(6):2279–2284

doi: 10.1210/en.2003-0128

Gene Expression, Secretion, and Autocrine Action of C-Type Natriuretic Peptide in Cultured Adult Rat Cardiac Fibroblasts

TAKESHI HORIO, TAKESHI TOKUDOME, TOSHIYUKI MAKI, FUMIKI YOSHIHARA, SHIN-ICHI SUGA, TOSHIO NISHIKIMI, MASAYASU KOJIMA, YUHEI KAWANO, AND KENJI KANGAWA

Department of Medicine (T.H., F.Y., Y.K.) and Research Institute (T.T., T.M., S.S., K.K.), National Cardiovascular Center, Suita, Osaka 565-8565, Japan; Department of Hypertension and Cardiorenal Medicine, Dokkyo University School of Medicine (T.N.), Tochigi 321-0293, Japan; and Institute of Life Sciences, Kurume University (M.K.), Kurume, Fukuoka 839-0861, Japan

C-type natriuretic peptide (CNP), the third member of the natriuretic peptide family, is known to be synthesized in the central nervous system and vascular endothelial cells, in contrast to atrial natriuretic peptide and brain natriuretic peptide. However, there have been no studies concerning CNP production in cultured cardiac cells. Here, we examined the production and the local effect of CNP in cultured ventricular cells. Under serum-free conditions, adult rat cardiac fibroblasts secreted immunoreactive CNP time dependently. TGF-β1, basic fibroblast growth factor, and endothelin-1 significantly stimulated CNP secretion. Northern blot analysis detected significant expressions of CNP and its specific receptor (guanylyl cyclase-B) mRNA in cardiac fibroblasts. CNP stimulated intracellular cGMP production in fibroblasts more intensely than atrial and brain natriuretic peptides. CNP inhibited both DNA and collagen syntheses of cardiac fibroblasts, and these inhibitory effects by CNP were stronger than by atrial and brain natriuretic peptides. The inhibition by CNP of DNA and collagen syntheses was reproduced by a cGMP analog, 8-bromo cGMP. The present findings demonstrate that CNP is synthesized in and secreted from cardiac fibroblasts and suggest that CNP has a suppressive effect on fibroblast proliferation and extracellular matrix production, probably via the guanylyl cyclase-B-mediated cGMP-dependent process. CNP produced by cardiac fibroblasts may play a role as an autocrine regulator against excessive cardiac fibrosis. (*Endocrinology* 144: 2279–2284, 2003)

THE NATRIURETIC PEPTIDES are a family of cyclic molecules that consist of three members, designated atrial natriuretic peptide (ANP), brain natriuretic peptide (BNP), and C-type natriuretic peptide (CNP; Ref. 1). ANP and BNP are primarily cardiac hormones secreted mainly from atria and ventricles, respectively. Once in the circulation, ANP and BNP bind to their specific receptors in the vascular tissue, kidney, and adrenal gland and induce vasodilatation, natriuresis, and diuresis. CNP, which was originally isolated from porcine brain extracts, not only acts as a neuropeptide in the central nervous system, but also plays a role in the local regulation of vascular tone, because CNP is synthesized in vascular endothelial cells (2).

Subsequent studies have revealed the existence of two biological [guanylyl cyclase (GC)-containing] natriuretic peptide receptors, called GC-A and GC-B, in cardiac cells (3). In addition to acting as a circulating hormone, therefore, ANP and BNP may have some function as autocrine and/or paracrine factors. In fact, some studies, including our *in vitro* study, showed that endogenous ANP and BNP suppress the development of cardiac myocyte hypertrophy and interstitial fibrosis (4–6). With regard to CNP, however, its production in cardiac cells and the local effect on the heart itself have remained to be elucidated. Therefore, we conducted this study to investigate the production of CNP and the expression of GC-B, a specific receptor for CNP, in cultured ventricular cells and to examine the effects of CNP on DNA and collagen syntheses by fibroblast cells.

Abbreviations: ANP, Atrial natriuretic peptide; bFGF, basic fibroblast growth factor; BNP, brain natriuretic peptide; CNP, C-type natriuretic peptide; FCS, fetal calf serum; GC, guanylyl cyclase; ir, immunoreactive.

Materials and Methods

Cell cultures

Adult rat cardiac fibroblasts were prepared according to a previously described protocol (7) with minor modifications. Apical halves of cardiac ventricles from 7-wk-old male Wistar rats were separated, minced, and dispersed with 0.1% collagenase type II (Worthington Biochemical Corp., Freehold, NJ). The isolated cells were resuspended in DMEM (Life Technologies, Inc., Grand Island, NY) supplemented with 10% fetal calf serum (FCS; Life Technologies, Inc.), and the suspension was plated onto 10-cm culture dishes for 2 h, which allowed for the preferential attachment of fibroblasts to the bottom of the culture dish. Nonadherent and weakly attached cells were then removed, and attached fibroblast cells were allowed to grow to confluence, trypsinized, and passaged 1:3 or 1:4. Adult cardiac fibroblasts at the second or third passage were used in the present study. The purity of cardiac fibroblasts and the absence of myocytes were confirmed by a morphological examination (fibroblasts are thin and triangular cells with light cytoplasm). In addition, the contamination of endothelial cells in our fibroblast culture was excluded by the lack of positive immunostaining with an antibody against von Willebrand factor (DAKO Corp. A/S, Glostrup, Denmark).

Neonatal ventricular myocytes and fibroblasts were prepared as described previously (8). From cardiac ventricles of 1- to 2-d-old Wistar rats, myocytes and fibroblasts were separately collected by the discontinuous Percoll gradient method. Primary cultures of neonatal rat car-

diac myocytes and neonatal cardiac fibroblasts at the second passage were used for the gene expression study.

Measurement of immunoreactive (ir-) ANP, BNP, and CNP

After adult cardiac fibroblasts were incubated for 12–72 h in 10-cm dishes with serum-free DMEM, the culture medium was collected. In the study examining the effect of various agents on ir-CNP secretion, cells were incubated for 24 h under treatment with IL-1β (Genzyme Techne, Minneapolis, MN), TNF-α (Sigma, St. Louis, MO), TGF-β1 (R&D Systems, Minneapolis, MN), basic fibroblast growth factor (bFGF; Sigma), IGF-1 (Sigma), insulin (Sigma), angiotensin II (Peptide Institute, Osaka, Japan), endothelin-1 (Peptide Institute), phenylephrine (Research Biochemicals International, Natick, MA), isoproterenol (Sigma), or norepinephrine (Research Biochemicals International). The collected medium (10 ml) was condensed with a Sep-Pak C18 cartridge (Waters, Milford, MA) and lyophilized. The RIA for rat ANP, BNP, and CNP was performed as previously reported (6, 9).

Characterization of ir-CNP

The conditioned medium (80 ml) from adult cardiac fibroblasts was condensed and separated by reverse-phase HPLC on a μ-Bondasphere C18 column (300 Å, 3.9 × 150 mm; Waters), as described previously (8). A linear gradient elution of acetonitrile for 10–60% in 0.1% trifluoroacetic acid was made at a flow rate of 1 ml/min, and each collected fraction (1 ml) was submitted for RIA for CNP.

Northern blot analysis

After incubation in DMEM with FCS, the cultured cells were rinsed with PBS and submitted for RNA extraction. Total RNA was extracted with TRIzol reagent (Life Technologies, Inc.) and poly(A)$^+$ RNA was prepared using Oligotex-dT30 Super (Takara Biomedicals, Shiga, Japan). Poly(A)$^+$ RNA (10 μg/lane) was electrophoresed on 1% agarose gel and then transferred to a nylon membrane. Hybridization and washing of the membrane were carried out with cDNA probes for rat CNP, ANP, GC-A, GC-B, and glyceraldehyde-3-phosphate dehydrogenase genes, according to the method previously reported (8, 9).

Measurement of cellular cGMP

After preincubation, adult cardiac fibroblasts grown in 24-well plates were treated for 10 min with various concentrations of synthetic ANP, BNP, or CNP (Peptide Institute) in the presence of 5×10^{-4} mol/liter 3-isobutyl-1-methylxanthine (Nacalai Tesque, Kyoto, Japan). The intracellular cGMP levels were determined by a RIA performed with a cGMP assay kit (Yamasa Shoyu, Chiba, Japan), as previously reported (6).

DNA and collagen syntheses

The effects of natriuretic peptides and a cGMP analog on DNA synthesis and collagen synthesis in adult rat cardiac fibroblasts were evaluated by the incorporation of [^{3}H]thymidine and [^{3}H]proline into cells, respectively, as described previously (10). Fibroblasts at the second or third passage were seeded at a density of 2.5×10^4 cells/well on 24-well plates. After incubation in DMEM with 10% FCS, subconfluent fibroblast cells (approximately 7.5×10^4 cells/well) were maintained in serum-free DMEM for 48 h. After the preconditioning period, the culture medium was replaced with fresh DMEM with 1% FCS. Then, ANP, BNP, CNP, or 8-bromo cGMP (Sigma) was added, and 0.5 μCi of [^{3}H]thymidine or [^{3}H]proline was also added. After the cells were incubated for 24 h, the radioactivity of aliquots of the trichloroacetic acid-insoluble material was determined using a liquid scintillation counter.

Statistical analysis

The significance of differences among groups was estimated by an unpaired ANOVA, and probability values were calculated by the Fisher method. A value of $P < 0.05$ was accepted as statistically significant.

Results

Secretion and characterization of ir-CNP in adult cardiac fibroblasts

The significant release of ir-CNP from adult cardiac fibroblasts into the serum-free medium was observed, and its level in fibroblasts increased in a time-dependent manner (Fig. 1A). Although the concentration of ir-ANP and ir-BNP in the same culture medium was also measured, the significant release of these peptides was not detected after 12–72 h of incubation.

Ir-CNP secreted from cultured fibroblasts was characterized by reverse-phase HPLC. Ir-CNP in the culture medium of adult cardiac fibroblasts consisted of one major and some minor components, and the major component was eluted at a retention time identical with that of authentic CNP (Fig. 1B).

We further examined which humoral factor stimulates CNP

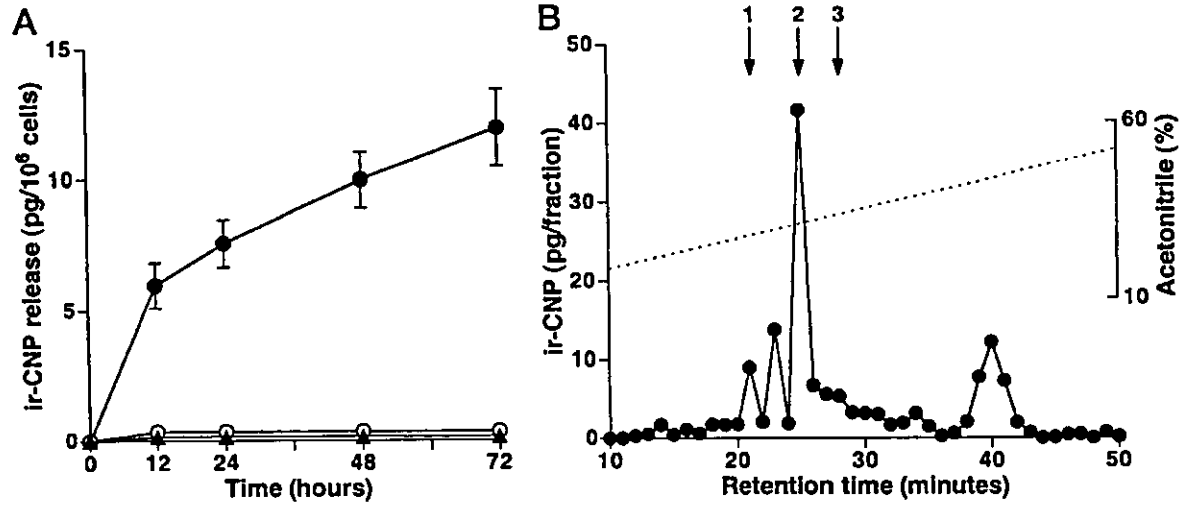

FIG. 1. A, Basal secretion of ir-CNP (●) from cultured adult rat cardiac fibroblasts under serum-free conditions. Values are mean ± SE of five measurements. Neither ir-ANP (○) nor ir-BNP (▲) was detected in the same culture medium. B, Reverse-phase HPLC analysis of ir-CNP in the culture medium of adult rat cardiac fibroblasts. *Arrows* indicate the elution positions of 1) ANP, 2) CNP, and 3) BNP.

release from adult cardiac fibroblasts. The secretion levels of ir-CNP were slightly but significantly increased by TGF-β1 (10^{-9} mol/liter) and bFGF (10^{-8} mol/liter) among several cytokines and growth factors (Table 1). Among vasoactive peptides and catecholamines, only endothelin-1 (10^{-7} mol/liter) stimulated the ir-CNP release from cardiac fibroblasts.

Expression of CNP and its receptor mRNA in adult and neonatal cardiac fibroblasts

By Northern blot analysis, a single band hybridizing to the rat CNP cDNA probe was found in adult rat cardiac fibroblasts at passages 2 and 3 (Fig. 2). The expression of ANP mRNA was not detected at all in the same membrane. We also investigated the CNP gene expression in cultured neonatal rat cardiac fibroblasts and myocytes. A weak transcript signal was observed in neonatal cardiac fibroblasts. On the other hand, no specific expression of CNP mRNA was found in neonatal cardiac myocytes, although strong gene expression of ANP was observed in those cells.

As for the expression of natriuretic peptide receptors, both GC-A and GC-B transcripts were found in adult and neonatal cardiac fibroblasts. However, expression levels of the GC-B receptor were much more intense than those of the GC-A in adult cardiac fibroblasts.

TABLE 1. Effects of various humoral factors on CNP secretion from adult cardiac fibroblasts

Factor	ir-CNP release (picograms/10^6 cells)
Control	6.0 ± 0.8
IL-1β (10 ng/ml)	7.4 ± 0.7
TNF-α (10 ng/ml)	7.4 ± 0.7
TGF-β1 (10^{-9} mol/liter)	9.0 ± 0.4[a]
bFGF (10^{-8} mol/liter)	9.8 ± 0.7[b]
IGF-1 (10^{-7} mol/liter)	7.1 ± 1.7
Insulin (10^{-6} mol/liter)	5.6 ± 0.4
Angiotensin II (10^{-7} mol/liter)	5.3 ± 0.6
Endothelin-1 (10^{-7} mol/liter)	9.9 ± 1.0[b]
Phenylephrine (10^{-5} mol/liter)	7.2 ± 1.2
Isoproterenol (10^{-5} mol/liter)	6.6 ± 1.7
Norepinephrine (10^{-5} mol/liter)	6.1 ± 1.4

Release levels were examined after 24 h of incubation. Values are mean ± SE of six measurements. [a] $P < 0.05$; and [b] $P < 0.01$ *vs.* control (vehicle alone).

Effects of natriuretic peptides on cellular cGMP production and on DNA and collagen syntheses in adult cardiac fibroblasts

CNP markedly increased the cellular level of cGMP in adult cardiac fibroblasts and its increase was concentration dependent (Fig. 3). Although ANP and BNP also increased the cGMP levels concentration dependently, the stimulation of cGMP formation by ANP or BNP was weaker than by CNP.

ANP, BNP, and CNP decreased the incorporation of [^{3}H]proline and [^{3}H]thymidine into adult cardiac fibroblasts (Fig. 4, A and B). Above all, CNP clearly inhibited collagen synthesis at concentrations of 10^{-10} mol/liter or greater, and DNA synthesis at concentrations of 10^{-9} mol/liter or greater,

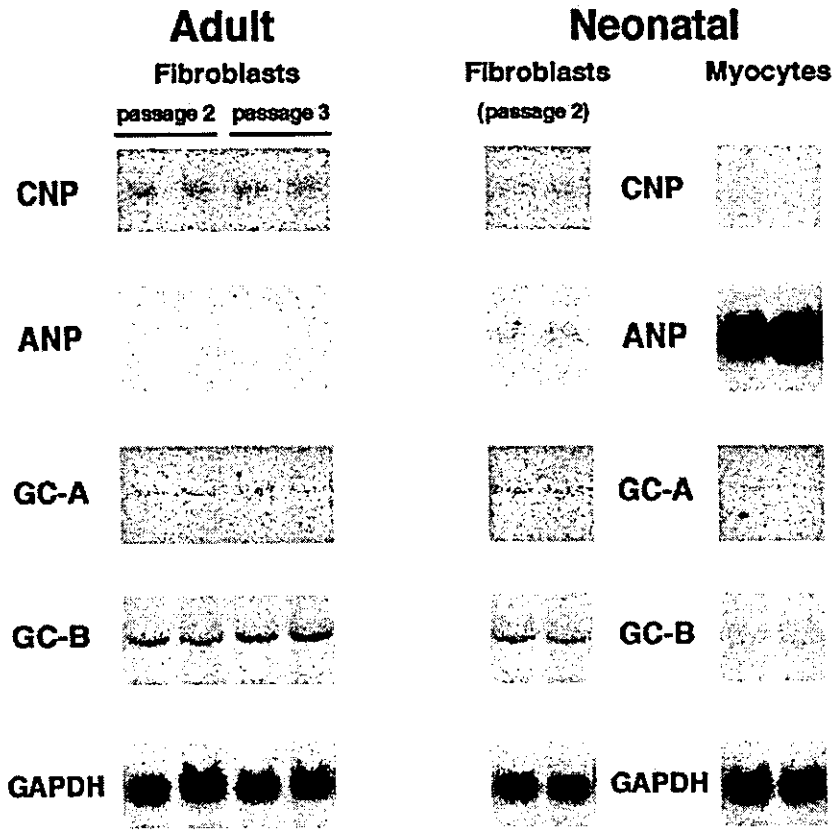

FIG. 2. The expression of rat CNP, ANP, GC-A, GC-B, and glyceraldehyde-3-phosphate dehydrogenase (GAPDH) mRNA in cultured adult rat cardiac fibroblasts (*left*) and neonatal rat cardiac fibroblasts and myocytes (*right*). Adult rat cardiac fibroblasts at the second or third passage, neonatal fibroblasts at the second passage, and primary cultures of neonatal cardiac myocytes were evaluated. The radioimages are representative of two separate experiments.

and these inhibitory effects of CNP were stronger than those of ANP and BNP. 8-Bromo cGMP, a membrane-permeable analog of cGMP, reduced both [^{3}H]proline and [^{3}H]thymidine incorporation in a dose-dependent manner (Fig. 4, C and D). Therefore, inhibition by natriuretic peptides of collagen and DNA syntheses in adult cardiac fibroblasts could be mimicked by this cGMP analog.

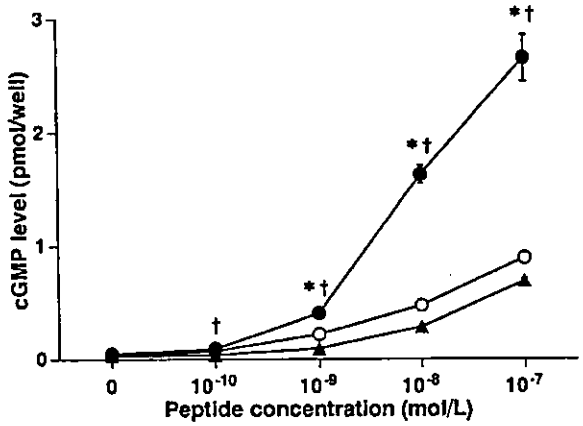

FIG. 3. Effects of ANP (○), BNP (▲), and CNP (●) on the production of cellular cGMP in cultured adult rat cardiac fibroblasts. Values are mean ± SE of four measurements. *, $P < 0.001$ *vs.* the same dose of ANP; †, $P < 0.001$ *vs.* the same dose of BNP.

Discussion

The present study has demonstrated for the first time that CNP is produced and secreted from cultured adult rat cardiac fibroblasts. Although CNP was initially thought to be distributed in the central nervous system and to act as a neuropeptide (1, 11), it has been shown that CNP is localized or synthesized in the kidney (12), bone (13), vascular cells (2, 14), and blood cells (15). As for the heart, discrepant findings have been reported. Some studies reported that ir-CNP or CNP mRNA was not detected in human or rat hearts (11, 16). On the other hand, Wei *et al.* (17) revealed the existence of CNP peptide in human ventricular myocardium by immunohistochemical staining. However, it does not necessarily indicate that CNP is synthesized in and secreted from cardiac myocytes. There is the possibility that the positive immunostaining of CNP by Wei *et al.* (17) might be attributable to the binding of CNP to its receptors, as they discussed. Vollmar *et al.* (18) and Minamino *et al.* (9) showed that CNP mRNA was detected in the rat heart using an RT-PCR technique. However, their studies have not clarified which type of cells synthesizes CNP in the heart. Moreover, the possi-

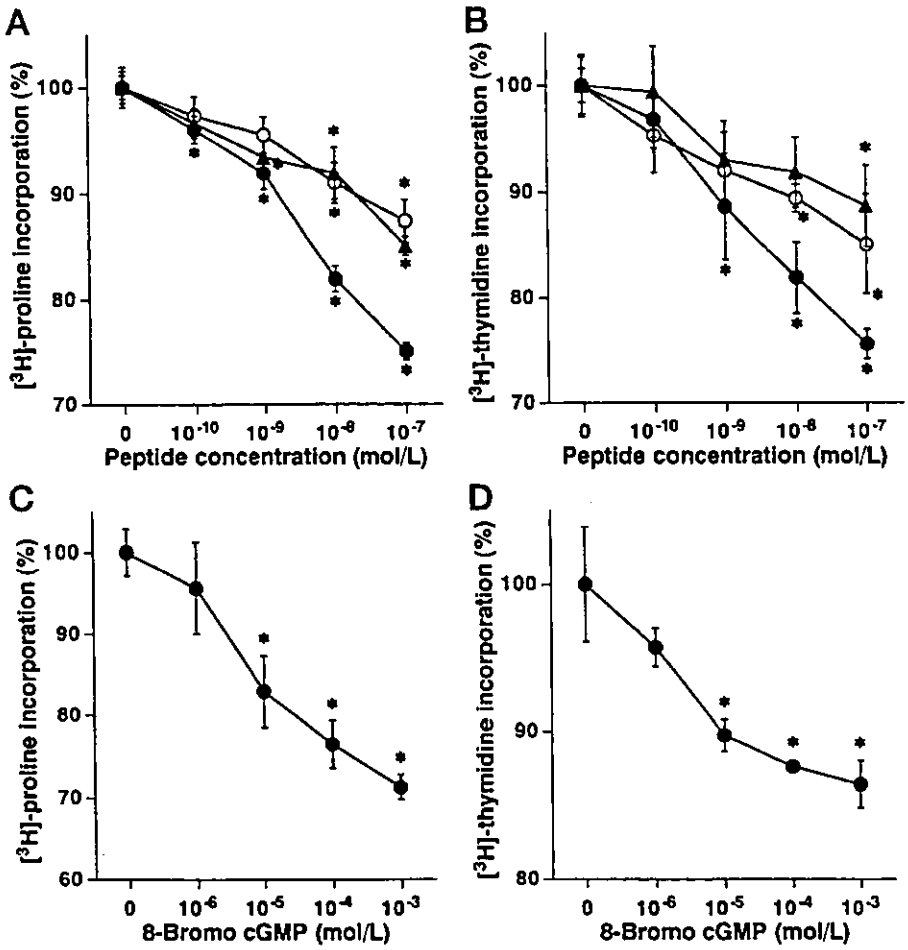

FIG. 4. Effects of ANP (○), BNP (▲), and CNP (●) on collagen synthesis (A) and DNA synthesis (B), and effects of 8-bromo cGMP on collagen synthesis (C) and DNA synthesis (D) in cultured adult rat cardiac fibroblasts. Values are percentages of control (mean ± SE of six measurements). Control represents proline or thymidine incorporation in cells incubated in DMEM with 1% FCS. The mean radioactivities in the control wells were 9,001 ± 135 (A), 10,402 ± 250 (B), 7,911 ± 233 (C), and 7,503 ± 291 cpm/well (D), respectively. *, $P < 0.05$ *vs.* control.

bility that the CNP gene expression was derived from coronary endothelium could not be ruled out, because the detection was induced by the RT-PCR method. In the present study, we demonstrated that cardiac fibroblasts, in which no contamination of endothelial cells was confirmed, secreted ir-CNP in a time-dependent manner. Although ANP and BNP were recently reported to be synthesized by cardiac fibroblasts (or myofibroblasts; Refs. 19 and 20), the HPLC profiles in the present study proved that the ir-CNP observed in the culture medium was not due to the cross-reactivity of ANP or BNP. In fact, neither ir-ANP nor ir-BNP was detected in the medium of cultured fibroblasts. Furthermore, we clearly showed by the Northern blot analysis the existence of CNP mRNA in adult and neonatal cardiac fibroblasts. Significant expression of the CNP gene was not observed in neonatal cardiac myocytes, although we failed to examine its expression in adult cultured cardiac myocytes. These findings suggest that CNP is produced probably only by cardiac fibroblasts, differing from the production site of ANP and BNP.

In the present study, TGF-β1, bFGF, and endothelin-1 among various humoral factors elicited a weak but significant stimulatory effect on CNP secretion. TGF-β and bFGF have been shown to increase CNP secretion in cultured vascular endothelial cells and/or chondrocytes (2, 13). In addition, it has been shown that CNP production is enhanced by activation of protein kinase C (21), of which endothelin-1 is one of the activators. Therefore, the present findings concerning stimulation factors of CNP secretion are consistent with previous observations. Because TGF-β1, bFGF, and endothelin-1 all increase collagen or DNA synthesis in cardiac fibroblasts, CNP induced by these factors may display a counter-action against cardiac fibrosis.

Previous studies showed that ANP and BNP inhibited collagen production and proliferation of cultured cardiac fibroblasts (22–24). However, little is known about the effect of CNP on those cells, except for one study reported that CNP as well as ANP and BNP decreased bFGF-induced DNA synthesis in neonatal cardiac fibroblasts (23). The present study has clearly demonstrated that CNP inhibits both DNA and collagen syntheses in adult cardiac fibroblasts, and that these suppressive effects by CNP are more potent than those by ANP or BNP. Furthermore, CNP increased the intracellular cGMP levels more markedly compared with ANP or BNP, and a cGMP analog reproduced the suppression of DNA and collagen syntheses. Three receptor subtypes for natriuretic peptides are presently known. Two of these receptors have GC activity (*i.e.* induce cGMP accumulation) and are called GC-A and GC-B. ANP and BNP bind specifically to GC-A rather than GC-B (25). In contrast, CNP binds to GC-B with a very high affinity but almost lacks the binding ability to GC-A (26). Because our study showed that cultured adult rat cardiac fibroblasts predominantly expressed the GC-B by Northern hybridization, the inhibitory effects of CNP on the proliferation and collagen production of cardiac fibroblasts are probably through a GC-B-mediated cGMP-dependent pathway. The present observations concerning the gene expression of the GC-B- and CNP-stimulated cGMP accumulation in fibroblasts were broadly consistent with the findings previously reported by Lin *et al.* (3). In their study, however, expression levels of the GC-A receptor in cultured cardiac fibroblasts were comparable to those of the GC-B, and ANP stimulated cGMP production as potently as CNP. The exact reason for such discrepant findings is unclear, but it may be partly due to the difference in the methods of preparation of cardiac fibroblasts and the conditions of the fibroblast cell culture used, including their purity and passages.

A previous study showed that GC-B mRNA levels were markedly increased in the hypertrophied left ventricle induced by volume overload (27). Furthermore, Doyle *et al.* (28) recently revealed that the distribution of the GC-B receptor in adult rat ventricles was confined to the nonmyocytes such as interstitial and vascular fibroblasts. These findings suggest that CNP released from cardiac fibroblasts may function effectively on themselves as an autocrine negative regulator against excessive cardiac fibrosis in pathological states. However, further investigations are necessary to clarify the physiological and pathophysiological roles of endogenous CNP in the heart.

In conclusion, the present study demonstrated that CNP was synthesized in and secreted from cultured adult cardiac fibroblasts and that CNP inhibited DNA and collagen syntheses in these cells more potently than ANP and BNP. Cardiac CNP produced by fibroblasts may function as a local modulator of cardiac fibrosis, defined as a proliferation of interstitial fibroblasts and the biosynthesis of extracellular matrix components.

Acknowledgments

We thank Yoko Saito for her technical assistance.

Received January 27, 2003. Accepted March 4, 2003.

Address all correspondence and requests for reprints to: Takeshi Horio, M.D., Division of Hypertension and Nephrology, Department of Medicine, National Cardiovascular Center, 5-7-1, Fujishirodai, Suita, Osaka 565-8565, Japan. E-mail: thorio@ri.ncvc.go.jp.

This work was supported by the Promotion of Fundamental Studies in Health Science of the Organization for Pharmaceutical Safety and Research of Japan, grants-in-aid for scientific research (14571044) from Japan Society for the Promotion of the Science, and U.S. Public Health Science Grants DK-52121 and HL-68607.

References

1. **Sudoh T, Minamino N, Kangawa K, Matsuo H** 1990 C-type natriuretic peptide (CNP): a new member of natriuretic peptide family identified in porcine brain. Biochem Biophys Res Commun 168:863–870
2. **Suga S, Nakao K, Itoh H, Komatsu Y, Ogawa Y, Hama N, Imura H** 1992 Endothelial production of C-type natriuretic peptide and its marked augmentation by transforming growth factor-β. Possible existence of "vascular natriuretic peptide system". J Clin Invest 90:1145–1149
3. **Lin X, Hänze J, Heese F, Sodmann R, Lang RE** 1995 Gene expression of natriuretic peptide receptors in myocardial cells. Circ Res 77:750–758
4. **Oliver PM, Fox JE, Kim R, Rockman HA, Kim HS, Reddick RL, Pandey KN, Milgram SL, Smithies O, Maeda N** 1997 Hypertension, cardiac hypertrophy, and sudden death in mice lacking natriuretic peptide receptor A. Proc Natl Acad Sci USA 94:14730–14735
5. **Tamura N, Ogawa Y, Chusho H, Nakamura K, Nakao K, Suda M, Kasahara M, Hashimoto R, Katsuura G, Mukoyama M, Itoh H, Saito Y, Tanaka I, Otani H, Katsuki M, Nakao K** 2000 Cardiac fibrosis in mice lacking brain natriuretic peptide. Proc Natl Acad Sci USA 97:4239–4244
6. **Horio T, Nishikimi T, Yoshihara F, Matsuo H, Takishita S, Kangawa K** 2000 Inhibitory regulation of hypertrophy by endogenous atrial natriuretic peptide in cultured cardiac myocytes. Hypertension 35:19–24
7. **Eghbali M, Tomek R, Sukhatme VP, Woods C, Bhambi B** 1991 Differential effects of transforming growth factor-β1 and phorbol myristate acetate on

cardiac fibroblasts. Regulation of fibrillar collagen mRNAs and expression of early transcription factors. Circ Res 69:483–490
8. **Horio T, Nishikimi T, Yoshihara F, Nagaya N, Matsuo H, Takishita S, Kangawa K** 1998 Production and secretion of adrenomedullin in cultured rat cardiac myocytes and nonmyocytes: stimulation by interleukin-1β and tumor necrosis factor-α. Endocrinology 139:4576–4580
9. **Minamino N, Aburaya M, Kojima M, Miyamoto K, Kangawa K, Matsuo H** 1993 Distribution of C-type natriuretic peptide and its messenger RNA in rat central nervous system and peripheral tissue. Biochem Biophys Res Commun 197:326–335
10. **Horio T, Nishikimi T, Yoshihara F, Matsuo H, Takishita S, Kangawa K** 1999 Effects of adrenomedullin on cultured rat cardiac myocytes and fibroblasts. Eur J Pharmacol 382:1–9
11. **Komatsu Y, Nakao K, Suga S, Ogawa Y, Mukoyama M, Arai H, Shirakami G, Hosoda K, Nakagawa O, Hama N, Kishimoto I, Imura H** 1991 C-type natriuretic peptide (CNP) in rats and humans. Endocrinology 129:1104–1106
12. **Suzuki E, Hirata Y, Hayakawa H, Omata M, Kojima M, Kangawa K, Minamino N, Matsuo H** 1993 Evidence for C-type natriuretic peptide production in the rat kidney. Biochem Biophys Res Commun 192:532–538
13. **Hagiwara H, Sakaguchi H, Itakura M, Yoshimoto T, Furuya M, Tanaka S, Hirose S** 1994 Autocrine regulation of rat chondrocyte proliferation by natriuretic peptide C and its receptor, natriuretic peptide receptor-B. J Biol Chem 269:10729–10733
14. **Woodard GE, Rosado JA, Brown J** 2002 Expression and control of C-type natriuretic peptide in rat vascular smooth muscle cells. Am J Physiol Regul Integr Comp Physiol 282:R156–R165
15. **Ishizaka Y, Kangawa K, Minamino N, Ishii K, Takano S, Eto T, Matsuo H** 1992 Isolation and identification of C-type natriuretic peptide in human monocytic cell line, THP-1. Biochem Biophys Res Commun 189:697–704
16. **Takahashi T, Allen PD, Izumo S** 1992 Expression of A-, B-, and C-type natriuretic peptide genes in failing and developing human ventricles. Correlation with expression of the Ca^{2+}-ATPase gene. Circ Res 71:9–17
17. **Wei CM, Heublein DM, Perrella MA, Lerman A, Rodeheffer RJ, McGregor CGA, Edwards WD, Schaff HV, Burnett Jr JC** 1993 Natriuretic peptide system in human heart failure. Circulation 88:1004–1009
18. **Vollmar AM, Gerbes AL, Nemer M, Schulz R** 1993 Detection of C-type natriuretic peptide (CNP) transcript in the rat heart and immune organs. Endocrinology 132:1872–1874
19. **Cameron VA, Rademaker MT, Ellmers LJ, Espiner EA, Nicholls MG, Richards AM** 2000 Atrial (ANP) and brain natriuretic peptide (BNP) expression after myocardial infarction in sheep: ANP is synthesized by fibroblasts infiltrating the infarct. Endocrinology 141:4690–4697
20. **Tsuruda T, Boerrigter G, Huntley BK, Noser JA, Cataliotti A, Costello-Boerrigter LC, Chen HH, Burnett Jr JC** 2002 Brain natriuretic Peptide is produced in cardiac fibroblasts and induces matrix metalloproteinases. Circ Res 91:1127–1134
21. **Yamada Y, Yokota M** 1996 Production of C-type natriuretic peptide in human aortic endothelial cells induced by activation of protein kinase C. Am J Hypertens 9:924–929
22. **Fujisaki H, Ito H, Hirata Y, Tanaka M, Hata M, Lin M, Adachi S, Akimoto H, Marumo F, Hiroe M** 1995 Natriuretic peptides inhibit angiotensin II-induced proliferation of rat cardiac fibroblasts by blocking endothelin-1 gene expression. J Clin Invest 96:1059–1065
23. **Cao L, Gardner DG** 1995 Natriuretic peptides inhibit DNA synthesis in cardiac fibroblasts. Hypertension 25:227–234
24. **Redondo J, Bishop JE, Wilkins MR** 1998 Effect of atrial natriuretic peptide and cyclic GMP phosphodiesterase inhibition on collagen synthesis by adult cardiac fibroblasts. Br J Pharmacol 124:1455–1462
25. **Suga S, Nakao K, Hosoda K, Mukoyama M, Ogawa Y, Shirakami G, Arai H, Saito Y, Kambayashi Y, Inouye K, Imura H** 1992 Receptor selectivity of natriuretic peptide family, atrial natriuretic peptide, brain natriuretic peptide, and C-type natriuretic peptide. Endocrinology 130:229–239
26. **Koller KJ, Lowe DG, Bennett GL, Minamino N, Kangawa K, Matsuo H, Goeddel DV** 1991 Selective activation of the B natriuretic peptide receptor by C-type natriuretic peptide (CNP). Science 252:120–123
27. **Brown LA, Nunez DJR, Wilkins MR** 1993 Differential regulation of natriuretic peptide receptor messenger RNAs during the development of cardiac hypertrophy in the rat. J Clin Invest 92:2702–2712
28. **Doyle DD, Upshaw-Earley J, Bell EL, Palfrey HC** 2002 Natriuretic peptide receptor-B in adult rat ventricle is predominantly confined to the nonmyocyte population. Am J Physiol Heart Circ Physiol 282:H2117–H2123

ELSEVIER

Cardiovascular Research 58 (2003) 231–238

Cardiovascular Research

www.elsevier.com/locate/cardiores

Potentiation of C-type natriuretic peptide with ultrasound and microbubbles to prevent neointimal formation after vascular injury in rats

Hiroto Takeuchi[a], Koji Ohmori[a,*], Isao Kondo[a], Akira Oshita[a], Kaori Shinomiya[a], Yang Yu[a], Yuichiro Takagi[a], Katsufumi Mizushige[a], Kenji Kangawa[b], Masakazu Kohno[a]

[a]*Second Department of Internal Medicine, Kagawa Medical University, 1750-1, Ikenobe, Miki-cho, Kita-gun, Kagawa 761-0793, Japan*
[b]*Department of Biochemistry, National Cardiovascular Center Research Institute, 5-7-1, Fujishirodai, Suita, Osaka 565-8565, Japan*

Received 6 September 2002; accepted 27 November 2002

Abstract

Objectives: Long-term intravenous infusion of high-dose C-type natriuretic peptide (CNP) is known to prevent neointimal formation after vascular injury. Ultrasound (US) irradiation during microbubbles (MBs) infusion (US/MBs) has been used for local delivery of bioactive agents. We examined whether short-term infusion of CNP could also inhibit neointimal development and whether combined US/MBs treatment at the beginning of the CNP infusion could enhance its effect. **Methods:** In the rat carotid artery-balloon injury model, the intima/media area (I/M) ratio 14 days after injury was compared among various short-term post-injury treatments. For combined US/MBs, a commercial echocardiograph (1.8 MHz, mechanical index 1.0) and albumin-coated octafluoropropane gas MBs were used. **Results:** Infusion of high-dose CNP (1.0 μg/kg/min) immediately after injury for only 24 h successfully reduced the I/M ratio (0.18±0.05) to 18% of the ratio in control rats (1.00±0.13) that underwent only balloon injury. Although low-dose CNP (0.1 μg/kg/min for 24 h) alone was not effective in reducing the I/M ratio (0.83±0.18), combined US/MBs treatment for the first 80 min of the infusion markedly reduced the I/M ratio (0.17±0.07), which persisted until 28 days after injury (0.16±0.04). **Conclusions:** The effects of CNP on the events occurring early after arterial injury may be important in preventing subsequent neointimal development. Thus, intravenous infusion of CNP with US/MBs at its initiation may provide a clinically feasible anti-restenosis therapy applicable immediately after vascular interventions.

Keywords: Natriuretic peptide; Receptors; Restenosis; Smooth muscle; Ultrasound

1. Introduction

Neointimal hyperplasia follows injury to the arterial wall as a result of migration and proliferation of smooth muscle cells (SMCs) [1,2] and/or bone marrow-derived smooth-muscle progenitor cells [3]. These processes lead to restenosis, one of the unsolved limitations of intravascular interventions [1–3]. Although a sirolimus-eluting stent that inhibits the proliferation of lymphocytes and SMCs has recently been shown to be promising [4], no effective therapy to prevent restenosis after non-stent angioplasty has yet been established.

C-type natriuretic peptide (CNP), first identified in the porcine brain, is the third member of the family of natriuretic peptides [5]. CNP is a secreted polypeptide consisting of 22 amino acids with a ring structure formed by an intramolecular disulfide linkage and binds to guanylate cyclase-linked natriuretic peptide receptor-B (NPR-B) [5,6]. In addition to their vasorelaxant and natriuretic effects, these peptides, especially CNP, can inhibit SMCs migration and proliferation through the cyclic guanosine 3′,5′-monophosphate (cGMP) cascade

*Corresponding author. Tel./fax: +81-87-891-2151.
E-mail address: komori@kms.ac.jp (K. Ohmori).

Time for primary review 31 days.

0008-6363/03/$ – see front matter
doi:10.1016/S0008-6363(02)00833-7

[7–9]. In fact, it has been shown that CNP increases cGMP concentrations in cultured vascular SMCs expressing NPR-B in a dose dependent manner [8] and that a continuous systemic administration of a relatively high dose of CNP prevents neointimal formation following arterial injury in animals [10,11].

Previous studies have demonstrated that ultrasound irradiation in the presence of microbubbles (US/MBs) can increase cell membrane permeability, so-called 'sonoporation'. This has been used to enhance transfection of genes or plasmid DNA [12–14], which subsequently produce proteins, when the transfection is established with the temporary use of US/MBs. However, it remains unclear whether short-term US/MBs treatment can also enhance the effect of CNP, which does not require intracellular delivery but demands a persistent high-dose infusion for 5 days to 2 weeks after arterial injury to inhibit neointimal proliferation [10,11]. In the present study, we investigated whether (1) combined US/MBs treatment can augment the effect of CNP on the cGMP production in cultured vascular SMCs; (2) short-term CNP infusion following balloon injury can also prevent neointimal formation; or (3) combined US/MBs with CNP infusion for a clinically feasible time period potentiates its effect in the rat carotid artery.

2. Methods

2.1. In vitro study

2.1.1. Preparation and treatment of cultured smooth muscle cells

SMCs isolated from young Sprague–Dawley rat thoracic aortas using the standard scraping technique were grown to confluence in RPMI 1640 medium containing 10% fetal calf serum, penicillin (100 μg/ml) and streptomycin (50 μg/ml), and were maintained at 37 °C with atmospheric air and 5% CO_2 [15]. These cells were identified by their typical morphological and growth characteristics. Monolayers of SMCs subcultured on 24-well cell culture plates between the 4th and 9th passages were washed twice with PBS, and then treated with various combinations of CNP, microbubbles (MBs), and ultrasound (US).

Human CNP-22 (Peptide Institute, Osaka, Japan) was used in this study. The amino acid sequence of CNP is identical in humans, pigs, and rats [5,16,17]. CNP was prepared in Hanks' balanced salt solution with 20 mM HEPES (pH 7.0) containing 1 mM 3-isobutyl-1-methylxanthine, and was used at a final concentration of 10^{-7} mol/l. A transpulmonary US contrast agent Optison® (Mallinckrodt Medical, St. Louis, MO, USA) that is a suspension of octafluoropropane-filled albumin microbubbles [18] was added to the solution at a final concentration of 2×10^7 microbubbles/ml. For US irradiation, an S4 transducer of the Sonos 5500 (Philips Medical Systems, Andover, MA, USA) was placed under the bottom of the culture plate via a 2-cm thick acoustic coupler. US at a transmission frequency of 1.8 MHz and a mechanical index of 1.0 was applied in second harmonic mode at a frame rate of 30 Hz for 60 s immediately after adding CNP and/or MBs to the medium. Ultrasound penetration through the bottom of the culture plate was confirmed by visualizing the suspension of MBs in a well of the plate using the same insonation as the treatment.

Six treatment combinations based on the presence (+) or absence (−) of CNP, MBs and US were compared: (1) CNP(−)MB(−)US(−); (2) CNP(−)MB(+)US(+); (3) CNP(+)MB(−)US(−); (4) CNP(+)MB(+)US(−); (5) CNP(+)MB(−)US(+); and (6) CNP(+)MB(+)US(+). Moreover, we examined the effect of the presence of MBs in the medium on the concentration of free CNP. A mixture of MBs and CNP at the same concentrations applied to cultured SMCs was centrifuged at 1500 rpm for 3 min. After removing the MBs fractions from a sample of the mixture, the CNP concentration in the remaining sample was measured using an enzyme-immunoassay kit (Phoenix Pharmaceuticals, Belmont, CA, USA).

2.1.2. cGMP measurement

The reaction was stopped at 5, 10, 15, and 30 min after its onset by rapid aspiration and the addition of 1 ml of 5% trichloroacetic acid. After centrifugation at 12 000 rpm for 5 min at 4 °C, the supernatant was collected and 1 N NaOH 250 μl was added. The cGMP concentrations were then measured using a cGMP enzyme-immunoassay system (Amersham Pharmacia Biotech UK, Buckinghamshire, UK) [8] by a person (KS) who was blinded to the treatment condition of each sample.

2.2. In vivo study

We designed an in vivo study employing the rat carotid artery balloon injury model [19] to determine the effect of short-term CNP infusion and its potentiation by US irradiation combined with MBs infusion to prevent neointimal formation. This study conforms to the *Guide for the Care and Use of Laboratory Animals* published by the US National Institutes of Health (NIH Publication No. 85-23, revised 1996).

2.2.1. Animal preparation

Male Sprague–Dawley rats, weighing 350–400 g, were used in the study. The 36 animals were anesthetized with an intraperitoneal injection of 50 mg/kg sodium pentobarbital. The right jugular and femoral veins were cannulated for infusion of CNP and MBs, respectively. A 2F Fogarty embolectomy balloon catheter (Baxter Healthcare, Irvine, CA, USA) was inserted through the left iliac artery and advanced to the left carotid artery via the aorta. After confirmation of the presence of the catheter in the common carotid artery by echography, mechanical injury